BRAIN TUMOR ANALYSIS AND CLASSIFICATION OF BRAIN MR IMAGES

BY

GHAZANFAR LATIF

A Thesis Presented to the

DEANSHIP OF GRADUATE STUDIES

KING FAHD UNIVERSITY OF PETROLEUM & MINERALS

DHAHRAN, SAUDI ARABIA

In Partial Fulfillment of the
Requirements for the Degree of

MASTER OF SCIENCE

In

COMPUTER SCIENCE

May, 2014

KING FAHD UNIVERSITY OF PETROLEUM & MINERALS

DHAHRAN- 31261, SAUDI ARABIA

DEANSHIP OF GRADUATE STUDIES

This thesis, written by **GHAZANFAR LATIF** under the direction his thesis advisor and

approved by his thesis committee, has been presented and accepted by the Dean of

Graduate Studies, in partial fulfillment of the requirements for the degree of   **MASTER**
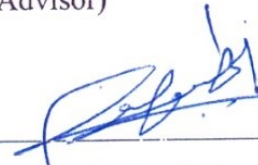
OF SCIENCE IN COMPUTER SCIENCE.

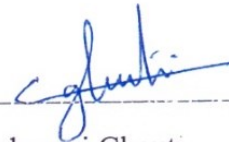Dr. Adel F. Ahmed
Department Chairman

Dr. Salam A. Zummo
Dean of Graduate Studies

3/6/14

Date

Dr. Sabri A. Mahmoud
(Advisor)

Dr. Wasfi G. Al-Khatib
(Member)

Dr. Lahouari Ghouti
(Member)

DEDICATION

I dedicate this dissertation with all of my
love to my parents, brothers and sisters.

ACKNOWLEDGMENTS

TABLE OF CONTENTS

LIST OF TABLES

LIST OF FIGURES

LIST OF ABBREVIATIONS

MRI	:	Magnetic Resonance Imaging
WHO	:	World Health Organization
3D	:	Three Dimensional
CT	:	Computer Tomography
DICOM	:	Digital Imaging and Communications in Medicine
PET	:	Positron Emission Tomography
T1	:	Longitudinal Relaxation Time
T2	:	Traverse Relaxation Time
PD	:	Proton Density
PCA	:	Principle Component Analysis
DWT	:	Discrete Wavelet Transform
DCT	:	Discrete Cosine Transform
DFT	:	Discrete Furious Transform
FCM	:	Fuzzy C-Mean
SVM	:	Support Vector Machine
KNN	:	K Nearest Neighbor
FPNN	:	Feed Forward Back Propagation Neural Network
BPNN	:	Backward Propagation Neural Network

PNN	:	Probabilistic Neural Network
ROI	:	Region of Interest
FGMM	:	Finite Gaussian Mixture Model
GHMRF	:	Gaussian Hidden Markov Random Field Model
GPV	:	Gaussian and Partial Volume Model
WM	:	White Matter
GM	:	Gray Matter
CSF	:	Cerebrospinal Fluid
CSA	:	Converging Square Algorithm
LoG	:	Laplacian of Gaussian
CWT	:	Continuous wavelet transform
ANN	:	Artificial Neural Networks
SWT	:	Semantic Web Technologies
SWRL	:	Semantic Web Rule Language
ECG	:	Electrocardiography

ABSTRACT

Full Name   : Ghazanfar Latif

Thesis Title   : Brain Tumor Analysis and Classification of Brain MR Images

Major Field   : Computer Science

Date of Degree : 17/05/2014

Magnetic resonance imaging (MRI) is a medical imaging modality frequently used to produce a pictorial view of inner body structure and functionality. Radiologists analyze large number of MR images for brain tumor detection. In MR images, various objects look similar in terms of shape, size and density. To properly deal with such similar objects, advanced image segmentation is required. Moreover, image segmentation, an important and effective tool in medical imaging, is used in the segmentation of lung, breast and brain images. On the other hand, brain tissues consist of cerebrospinal fluid, gray matter and white matter. In brain MRI, it is a difficult process to recognize and separate these tissue regions due to similarity, noise, and other factors.

This thesis aims at conducting a research in the area of brain tumor segmentation and classification.

The thesis findings will help medical practitioners in analyzing brain MRI scans for the detection of brain tumors. To achieve this goal, brain MR images are analyzed using segmentation and classification based on existing and proposed techniques. The proposed segmentation and classification techniques outperform the existing ones in terms of accuracy.

The proposed techniques extract first brain parts from MR images. Then, features are extracted from these parts using discrete cosine, discrete Fourier and discrete wavelet transforms. Features extracted using the latter transform are further reduced using the principle component analysis (PCA) algorithm. Finally, the extracted features are classified using support vector machines, naïve Bayes, multilayer perceptron and k-nearest neighbor classifiers. Unlike existing segmentation and classification techniques, the proposed ones attained the highest accuracy levels using all the assessed classifiers.

ملخص الرسالة

الاسم الكامل: غضنفر لطيف

عنوان الرسالة: تحليل و تصنيف صور الرنين المغناطيسي لأورام الدماغ

التخصص: علوم الحاسب الآلي

تاريخ الدرجة العلمية: مايو ٢٠١٤

التصوير بالرنين المغناطيسي (MRI) هو طريقة تصوير طبي شائعة الإستخدام للحصول على رؤية تصويرية لبنية الجسم الداخلية و الوظيفية.

كما يقوم أخصائيو الأشعة بتحليل عدد كبير من صور الرنين المغناطيسي للكشف عن أورام في المخ.

تبدو أشياء متغايرة متشابهة من حيث الشكل والحجم و الكثافة في صور الرنين المغناطيسي مما يستوجب إستخدام تقنيات التجزئة (segmentation). و لهذا أصبحت تقنيات التجزئة أداة هامة وفعالة في المجال التصوير الطبي، وهي تستخدم في كثيرا لمعالجة صور الرئتين والثدي و الدماغ. و من ناحية أخرى فإن أنسجة المخ تنقسم إلى ثلاثة أنواع رئيسية : السائل النخاعي، والمادة الرمادية و المادة البيضاء. كما يتسم التصوير بالرنين المغناطيسي للدماغ بصعوبة التعرف و فصل مناطق هذه الأنسجة بسبب التشابه و متويات الإشارات المتداخلة (additive noise)، الخ.

تهدف هذه الرسالة لإجراء بحث في مجالي تجزئة وتصنيف أورام المخ للمساعدة في تحليل فحوصات الرنين المغناطيسي للمخ و مساعدة الأطباء والباحثين في الكشف عن أورام الدماغ. و لهذا

قمنا بتحليل الصور المخ تجزئة وتصنيف الجمجمة والدماغ و أورام الدماغ. كما تم الإستعانة بتقنيات شائعة الإستخدام لتجزئة وتصنيف للأورام، بلإضافة إلى تقنيات جديدة مقترحة في هذه الرسالة. و اتسمت التقنيات المقترحة بالدقة العالية في التجزئة والتصنيف مقارنة مع التقنيات المعروفة.

تقوم تقنيات التجزئة والتصنيف المقترحة بتحديد أجزاء الدماغ من صور الرنين المغناطيسي و استخدامها كأساس لاستخراج علامات مميزة باستخدام تحويل الجيب الرقمي، و تحويل الطيفي لفورير (Fourier)، تحويل المويجات الرقمي المعتمد على مبدأ التحليل على أساس العناصر الأساسية (PCA) لإختزال حجم العلامات المميزة. كما تم إستعمال مصنفات عدة باعتكاد كل من آلات أشعة الدعم (support vector machines)، تقنية بايز (Bayes) الساذجة، الشبكات العصبية الصناعية المتعددة الطبقات (multilayer perceptron) و الجار الأقرب لتقييم تقنيات التجزئة والتصنيف المقترحة. و أثبت هذا التقييم تحسنا كبيرا في الدقة مع كل المصنفات باستخدام جميع أنواع أجزاء المخ بالمقارنة مع صور الرنين المغناطيسي الغير معالجة.

CHAPTER 1

INTRODUCTION

A brain tumor is an abnormal growth of brain cells, which is one of the most common causes of death (Singh et al., 2003). According to the International Agency for Research on Cancer's report, cancer is the cause of death for more than 7.6 million people in 2008; this accounts for 13% of the total deaths worldwide for the same year (Ferlay et al., 2010). This report was published in 2013, and the number of deaths is still increasing. As per World Health Organization's (WHO) report, an estimated 22.2 million people will have developed cancer by the year 2030 (Omolara, 2011). Developing countries like Ghana, Kenya, Afghanistan, and similar countries would be facing the worst, where nearly 70% of the overall deaths worldwide are estimated to occur in these countries.

There are two main types of brain tumors: benign and malignant. Benign tumors are considered harmless while malignant tumors cause brain cancer. Magnetic Resonance Imaging (MRI) is an advanced medical imaging modality used to diagnose and interpret various parts of the body. Brain MRI is an advanced image modality which requires a number of sequences for proper interpretation of normal brain tissues and affected brain tissues. Nearly 150 to 300 MRIs are normally extracted through the powerful magnetic field of the MRI machine. Doctors usually require 30 to 45 minutes for the interpretation of brain MRI scans, depending on the kind of suspected phytology. Only few radiologists can do proper interpretation of brain MRIs, especially in developing countries

(Berrington de González & Darby, 2004). It is very difficult to diagnose a tumor in its initial state because of the overlapping hard tissues in the brain. These tissues tend to appear like a tumor which mislead a radiologist.

Our research will enable radiologists to utilize a system where they can form an opinion. The system's opinion is based on the clear classification, segmentation, and 3D visualization. If the system is implemented on a large scale, it is going to benefit the masses. It would eliminate most of the problems that prevent diagnosing the tumor at an early stage. If the system works in a collaborative environment all over the world, we would be able to develop a semantic knowledge base, based on the accuracy of brain tumor cases. This would not only help to manage the cases but also provide assistance to radiologists who are new to the field.

Image segmentation has become an important and effective tool in the medical field, as seen in medical tests such as lung CT-Scan image segmentation, breast MR image segmentation, and brain MRI segmentation (Martinez-Möller et al., 2009). The human brain has three major types of tissues: gray matter, white matter, and cerebrospinal fluid (Salat et al., 2011). In MRIs, it is a difficult process to recognize and separate these different brain tissue regions due to their similarity. In this research, our main focus is on segmenting the brain images and classifying them into healthy and tumorous.

For segmentation, we will introduce state-of-the-art techniques, implement suitable ones, and probably improve them. In the classification phase, we will use machine learning, neural networks, and digital image processing techniques.

1.1   Problem Statement

The brain is a very complex part of the human body which contains billions of neurons to process information and operates different body organs. The human brain has three parts: the cerebrum, the cerebellum, and the brainstem (Volpe, 2009). The brain is shielded by a protective skull which prevents direct damages and injuries to the brain. Figure 1 shows the complete anatomy of the human brain.
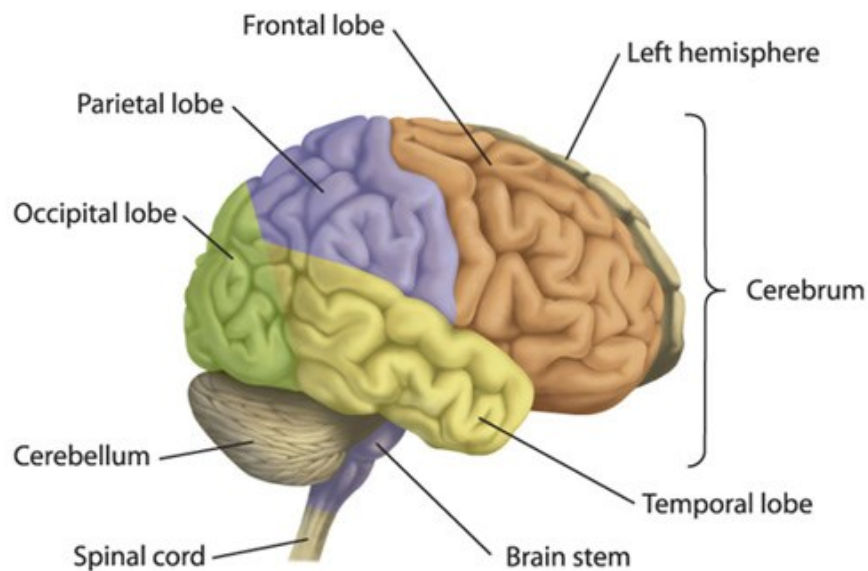
Figure 1: Human Brain Structure.

The brain is protected by the skull, but it still can be affected by internal neurological changes or damages. The most common problem is known as tumors. These damage the brain cells and have become the leading cause of death across the world. Figure 2 shows damaged brain cells and inflammation across the tumor's cells.
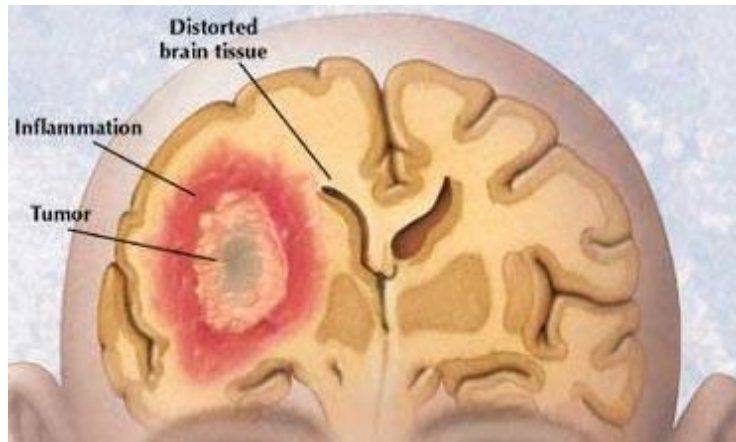
Figure 2: Brain Tumor.

Images are important in the field of medicine. X-ray images, MR images, and CT images are routinely used in hospitals. The development of medical imaging is rapidly moving towards more advanced computer utility. Today, many radiology departments are switching from traditional film handling to complete medical imaging (Choong, Logeswaran, & Bister, 2007).

There are several advantages to using medical imaging. First, it speeds up the analysis workflow where images are produced more quickly. Also, there is no need to archive films of medical images (Chad Stickrath, 2012). In addition, the computer provides possibilities to improve the usefulness of the images.

The automated analysis of brain tumor from MR images encompasses the following steps.

    I.   Scan object brain through MRI machine

   II.   Extracting brain MR images in DICOM format

  III.   Preprocessing brain MR images

  IV.   Extracting of skull and brain from the MR image

V.   Classifying of the extracted MR images into normal and abnormal images

VI.   Detecting of the brain tumor from the abnormal images

VII.   Visualizing of the brain tumor

VIII.   Decision Making

Figure 3 shows the diagram of the automated brain tumor analysis system.

MRI Scanning through MRI Machine

Brain MRI Scans in DICOM Format

Preprocessing Brain MRI Scans

Brain Image Segmentation

Brain Tumor Visualization

2D Brain Tumor Detection

Brain MRI Classification

Decision Making
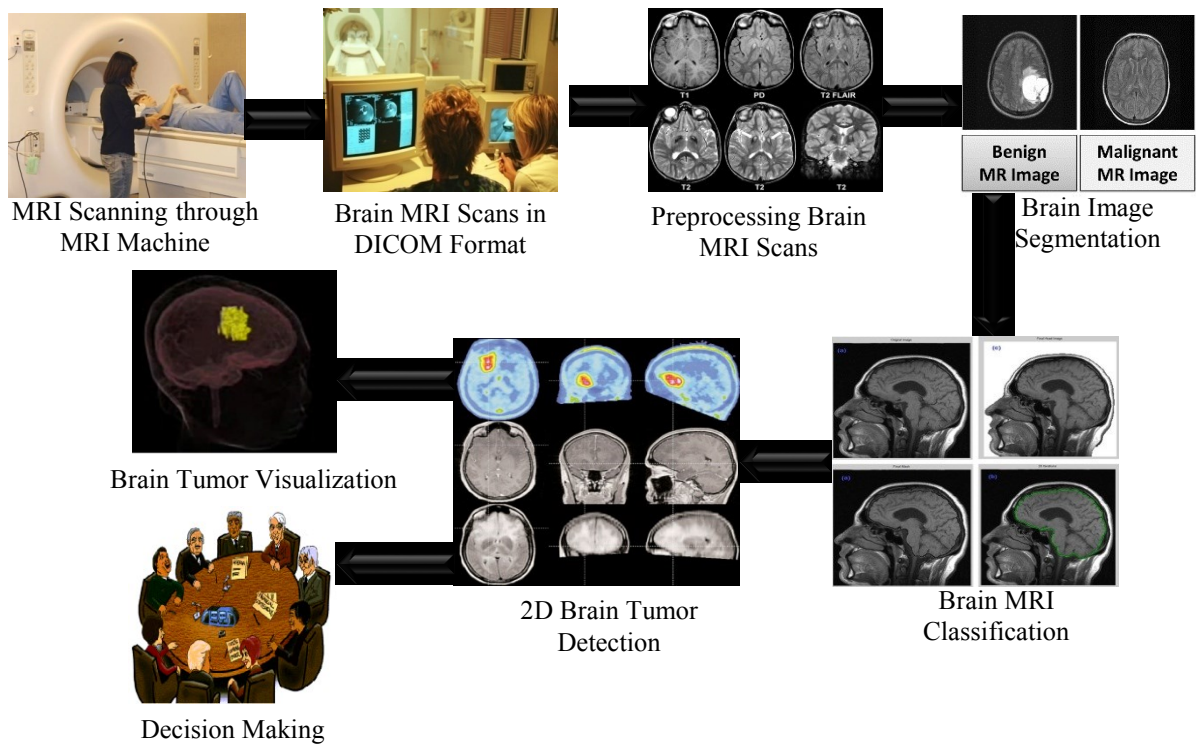
Figure 3: Architecture of brain tumor detection system.

1.2   Background and Motivation

Brain segmentation is a very important task due to the complex anatomy of the brain's structure and the skull. Most brain MR scans are highly correlated and low contrast,

which make segmentation more difficult. Correct segmentation of MRI plays a significant role for a meaningful analysis because most MR images are low contrast images, and brain tissue classes can easily overlap (Pichler, Kolb, Nägele, & Schlemmer, 2010). The complexity and inconsistency of the brain anatomy makes the MR image segmentation more difficult.

- Accurate brain image segmentation from MR images is a very important task for tumor analysis and treatment.

- Manual segmentation by experienced radiologists is a time-consuming and expensive process (Barkhausen et al., 2001).

- Manual brain and tumor segmentation is a subjective process, and the segmentation result varies among expert to expert.

- Tumors can be found at any location, with varying shape and size inside the brain, so automatic segmentation is a very challenging task.

1.3   Contribution

In this thesis we conducted research on brain tumor segmentation and classification from Brain MRI scans. Following are the contribution of the thesis.

1. We reviewed the state-of-art research in brain tumor segmentation and classification.

2. We gathered brain MRI data from different resources available to the research community, along with their achieved results.

3. We conducted research in the area of brain tumor analysis and classification. This will help the doctors and researchers in analyzing brain MRI scans and detecting brain tumor.

4. We analyzed and compared existing brain tumor analysis and classification techniques and applied new techniques/modified existing ones for brain analysis and classification.

5. We build a prototype system for the automated analysis of skull, brain, and brain tumor, as well as classification of brain tumor images.

1.4   Methodology

Brain tumor analysis and classification of brain MR images is a multi-step process consisting of MRI image acquisition, preprocessing, segmentation, feature extraction, feature selection, and classification. The following methodology is being followed during the thesis in order to achieve the proposed goals.

1. Extended the literature review of the state-of-art research in brain tumor analysis and classification, focusing on segmentation of the skull, the brain, and tumor, and classification of benign and malignant MR images.

2. Preprocess the acquired MRI datasets to convert them from DICOM format to bitmap image file format and remove embedded sample metadata in the MR images.

3. In the segmentation phase, we performed the following operations on the images:

a. Noise removal from the input MR image;

b. Extraction of the skull from the image and background removal;

c. Apply image enhancement and smoothing;

d. Initial segmentation of brain part in the image; and

e. Improve the segmented brain part.

4. In the feature extraction phase, we extracted brain MRI features from the MR images. We applied popular features of brain MR images.

5. In the classification phase, we applied statistical and machine-learning classifiers for brain tumor classification.

6. Based on the classification phase we separate the tumor from the malignant MR images using segmentation.

The proposed process model is illustrated in Figure 4.
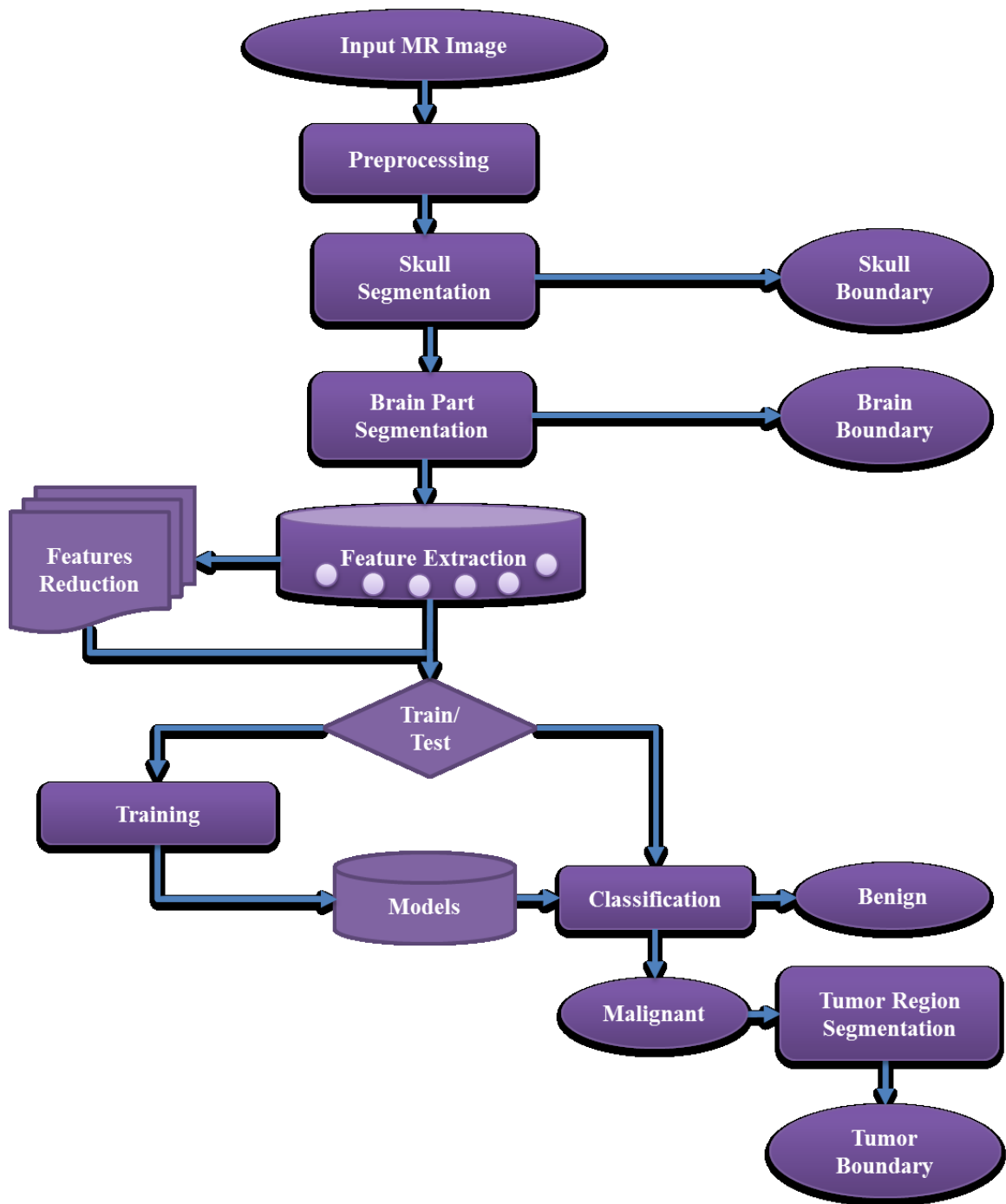
Figure 4: Proposed model of brain tumor detection.

1.5   Thesis Organization

Thesis is organized into seven chapters. The first chapter features a basic introduction on brain imaging issues and gives a comprehensive overview of the thesis. In the second chapter, we discuss the background of medical image processing and available techniques, while we also discuss the data acquisition that is used in latest existing literature. The third chapter gives a literature review about brain image segmentation and classification techniques. In this chapter, we discuss the latest literature and the new techniques used in them. The fourth chapter describes the preprocessing and brain part extraction techniques. In this chapter, we discuss different brain segmentation techniques and compare the results. In the fifth chapter, we present the feature extraction and reduction techniques. The sixth chapter describes the different classification methods used for brain MR image classification. In this chapter, we apply a number of classification techniques on the simulated datasets as well as real datasets, and compare the results. In the seventh chapter, we discuss our experimental results of proposed methods and conclude the dissertation with future directions.

CHAPTER 2

BACKGROUND

Image segmentation divides images into parts based on the properties of an image, such as gray level, texture, and shape of the different objects in the image. Segmentation is an unsupervised method which is used for extracting different regions having similar properties.

Image segmentation is very important for several medical image processing applications that are being used for the analysis of image structure and diagnosis of different disorders. Different segmentation and classification techniques are presented by the researchers.

2.1 Medical Image Modalities

There are four techniques commonly used for medical image modalities.

2.1.1 X-Rays

X-Rays or X-Radiation are primarily used to produce images of the body's internal structure. In this technique, electromagnetic radiation with different rates are being passed through the body to produce radiographic images with the help of an X-ray tube (He, Huda, Magill, Tavrides, & Yao, 2011). The soft parts of the body, such as the brain and the heart, show up as dark in the image, while bones and other dense parts of the

body appear as white in the images. X-Ray is commonly used for bone structure imaging, chest radiographs, lung cancer, brain tumor, and kidney stones identification, and skeletal system imaging.

2.1.2 Computer tomography Scan (CT-Scan)

CT-scan, also known as computed tomography, is a medical imaging technique used to produce two-dimensional images of the body. A CT scanner emits a series of electromagnetic radiation just like X-ray machines do, but the difference is that X-rays send only one beam while CT scan sends multiple beams (Fung Kon Jin et al., 2011). CT-Scan can be used for the head, brain, chest, abdomen, and cardiac images for analysis and identification of particular diseases.

2.1.3 Positron Emission Tomography (PET)

Positron emission tomography (PET) is a medical imaging method used to get information on how body tissues and organs are working based on three-dimensional images of the body. PET scan is different from other medical imaging techniques like MRI, X-ray, and CT-scan in terms of its feature: a PET scan is based on the cellular-level changes occurring in the organ or tissues, which then produces 3D images (Toma-Dasu et al., 2012). It can be used for the detection and monitoring of different diseases like cancer, brain disorders, and heart problems.

2.1.4 Magnetic resonance imaging (MRI)

Magnetic Resonance Imaging (MRI) is primarily a medical imaging technique most commonly used in radiology to visualize the internal structure and functionality of the body. An MRI machine contains a powerful magnet which works along with neutrons

and protons dipole moment. It generates detailed anatomical information of soft tissues in humans (Hyare et al., 2010). An MRI scan can be used for disease detection, and has proven successful in detecting heart abnormalities and brain tumors.

2.2   Brain MRI

Brain MRI is a test that uses magnetic field, radio waves, and a computer device to produce detailed images of the brain tissues and the brain stem. Three different types of brain MR images are produced based on the MRI signal frequency and magnet field strength: longitudinal relaxation time (T1) weighted, transverse relaxation time (T2) weighted, and proton density (PD) weighted (Foster-Gareau, Heyn, Alejski, & Rutt, 2003). These three different types of MR images are produced by using different pulse orders and by altering the imaging constraints. In MR images, tissues with T1 are dark, tissues with T2 are bright and tissues with PD shows water and macromolecules more clearly (de Leeuw et al., 2001). MRI uses magnetic field instead of radiation, which makes it a different technique from the CT scan. The MRI can detect swelling, tissue inflammation, bleeding, and tumor. MR scanned images can be saved into the computer for further evaluation.

| Object placed at moveable bed | For Brain MRI, head is scanned | MRI Scanner realigns hydrogen items | Released energy signal are being captured | From signals brain images are generated |
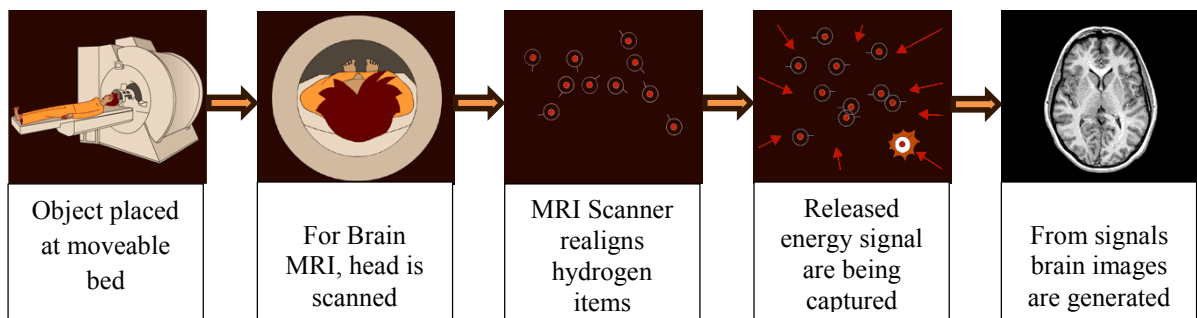
Figure 5: MR image capturing process from MRI Scanner.

2.3   Brain Cancer

Brain cancer (or brain tumor) occurs when brain cells reproduce and grow in an abnormal and uncontrolled manner. Kohler et al. divided brain tumor into two main categories (Kohler et al., 2011). The first one is benign tumors which remain separate from the brain's primary cells; these tumors are less serious but can still cause serious problems in the brain when they grow. The second type is malignant brain tumors which affect the primary brain cells and cause brain cancer. This type of brain tumors grow very quickly and damage primary brain cells.
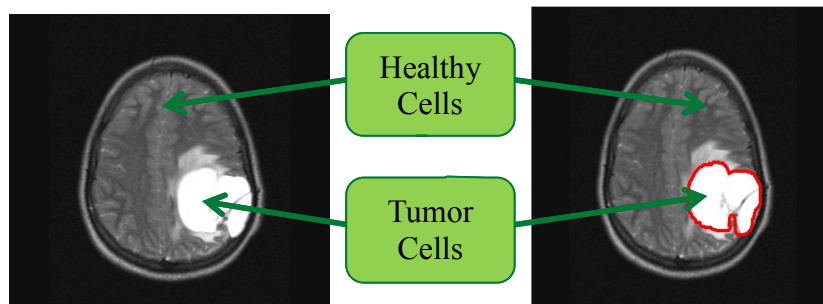
Figure 6: Normal and tumorous brain cell in MR images.

2.4   Data Acquisition

For the brain biomedical information and patients' MRI data, we contacted the Department of Radiology, Pakistan Institute of Medical Sciences, Islamabad, and received the data (Zehra et al., 2003). For biomedical information and understanding of MRI scans, we were in touch with Dr. Shazia Faruqui Khan (MBBS, FCRS London, and Associate Professor), currently working as Head of the Radiology Department in Pakistan

14

Institute of Medical Sciences, Islamabad. We were also in contact with Dr. Syeda Fizza Tauqir (MBBS, Nishter Medical College Multan and Post Graduate in Radiology, RMC Rawalpindi), who is a Radiologist at the Holy Family Hospital, Rawalpindi, for understanding the detection of brain tumor and analyzing the results. Dr. Mirza Aqeel, who is MRI Administrator at Abrar CT & MRI Centre, Rawalpindi helped us by providing Brain MRI Datasets of different patients (Abrar MRI, 2013). The acquired 8 datasets were scanned on a Philips Achieva 1.5T SE MRI scanner (Raaymakers et al., 2009).

We also downloaded recognized MRI datasets available online for research purpose published by Harvard Medical School (Pang & Lee, 2008). We extracted another brain tumors database of 10 cases from the Slicer 3.6; each case contains 123 MR images (Kikinis & Pieper, 2011). We also downloaded available online BRAINIX brain tumor database, which contain 7 subjects with MR images of T1 and T2 types (Rosset, Spadola, & Ratib, 2004). We also downloaded simulated brain MRI dataset consisting of 187 images from the BrainWeb online repository of simulated brain database (Ocosco, Ollokian, Wan, Ike, & Vans, 1996). The collected MRI data is described in Table 1.

2.5   Equipment Used

No special equipment is required for development and testing of MR images. However, we used a dedicated computing machine (laptop) with 12GB of memory and 2.20GHz i7 processor for application development and processing. We used MATLAB 7.11 (2012b) for coding and experiments (MathWorks, 2012). For preprocessing of DICOM images,

we used open source applications called Slicer 3.6 (Kikinis & Pieper, 2011) and
YAKAMI DICOM Tools (YAKAMI, 2012).

Table 1: Brain MRI Dataset Description.

Data Source	MRI Type	Slice Thickness (mm)	Number of Samples	Number of Images in each Sample
Pakistan Institute of Medical Sciences (Zehra et al., 2003)	T1, T2	5.0	8	190 to 210 Scans
Simulated BrainWeb Dataset (Ocosco et al., 1996)	T1	5.0	1	187 Scans
Slicer Brain MRI Repository (Kikinis & Pieper, 2011)	T2	1.5	10	123 Scans
BRAINIX Brain Tumor Dataset Repository (Rosset et al., 2004)	T1	1.5	7	22 Scans
Annotated Simulated BranWeb Dataset (Center, 2010)	T1	5	20	3 Scans
Annotated Simulated BranWeb Another Dataset (Ocosco et al., 1996)	T1	5	1	181 Scans
Abrar MRI & CT Scan Center (Abrar MRI, 2013)	T1	5.0	1	90 Scans

CHAPTER 3

LITERATURE REVIEW

In this section, we present the literature review on brain tumor segmentation and classification. We discuss an overview of the most commonly used segmentation, features extraction, selection methods, and classification techniques for brain MRI classification and segmentation. In addition, we explore the characteristic of brain MR images.

3.1   Features Extraction and Classification

Features extraction is the transformation of an image into a set of features. Good and nominal features play an important role in the accuracy of the classification technique. These features are further reduced to get only useful features which are used for image classification. A number of features extraction techniques are being proposed e.g. Gabor features (Manjunath & Ma, 1996; Liu & Wechsler, 2002; Kong, Zhang, & Li, 2003), wavelet transform-based features (Materka, 2001; Ma & Manjunath, 1995), a principle component analysis (PCA), discriminant analysis, and texture features (Materka & Strzelecki, 1998; H. Zhang, Fritts, & Goldman, 2005; Kovalev, Kruggel, Gertz, & von Cramon, 2001) in latest researches. Chaplot, et al. proposed feature extraction method based on wavelet transform (Duta & Sonka, 1998). A powerful mathematical tool called wavelets decomposes data into various frequencies that are used for the analysis and

classification of composite brain MRI datasets. Duabechies-4's wavelet approximation coefficients of brain MRI were extracted and used as feature vectors for classification (M. Flaum, M. Sonka, S. Arndt, T. Cizadlo, S. Stoneall, 1995). Principle component analysis is an important technique used for reduction of features into a lower dimension feature space. Dahshan extracted features using discrete wavelet transform and applied PCA to get lower dimensions of the feature space from brain MR images (El-Dahshan, Hosny, & Salem, 2010).

Xu et al. extracted features based on a linear separability criterion (Xu & Song, 2008) which is based on the Fisher discriminant analysis. This technique extracts features from data with complex or normal distribution. An improved version of discrete wavelet transform is called Slantlet transform. Madhubanti proposed a hybrid multi-resolution slantlet transform technique for feature extraction of brain MR images. She applied different filters for each scale of MR image and extracted the features. Quratulain extracted brain MRI features by using texture analysis (Quratulain, Latif, Kazmi, Jaffar, & Mirza, 2010). She used first-order features such as mean, skewness, variance, entropy, energy, and kurtosis, along with second-order features like inertia, max probability, and correlation. First order features were obtained from the histogram of the brain MR image, while second order features were extracted from the gray level spatial co-occurrence matrix.

Classification is a method for identification and categorization of input dataset into different classes. There are two basic types of classification known: the supervised classification and the unsupervised classification. Supervised classification is a method used to classify unknown samples by using samples of known identity, whereas

unsupervised classification is the identification of different patterns or natural groups without prior knowledge about the sample datasets. Numbers of supervised and unsupervised classification techniques are being utilized recently for brain image classification into benign and malignant. Zhang, et al. proposed a hybrid method for brain MRI classification (Yudong Zhang, Dong, Wu, & Wang, 2011). In their proposed method, two supervised classifiers k-nearest neighbor and feed forward back propagation artificial neural network have been developed. In a developed system, level-3 decomposed 1024 features were given as input while 10 hidden neurons were used to classify the MR image into a normal or an abnormal image. Fuzzy c-mean (FCM) clustering is also an important classification technique which classifies input patterns based on similarity and dissimilarity in the input patterns. Alan Liew proposed FCM clustering based on the adaptive classification of brain MR images (Liew & Yan, 2006). He incorporated the local spatial context into FCM using the dissimilarity index instead of distance matrix, and designed cluster prototype by applying a multiplicative bias field. Yang, et al. enhanced the improved brain MRI classification by applying a multi-scale multi-block FCM method (Yang & Fei, 2011).

Table 2: Summery of Brain MRI classifications techniques.

Author(s)	Features	Classification	Data	Accuracy (%)
Kaus et al. (Kaus et al., 2001)	DWT	SVM	52 MR Images (6 Normal, 46 Abnormal)	98%
Liew et al. (Liew & Yan, 2006)	Gradient Features	FCM	217 MRI Scans	-
Maitra et al. (Maitra & Chatterjee, 2008)	Multi Resolution Slantlet	FCM	75 MR Images (39 Normal, 36 Abnormal)	100%
El-Dahshan et al. (El-Dahshan et al., 2010)	DWT + PCA	Hybrid (KNN, FPNN)	70 MRI Scans (60 Normal, 10 Abnormal)	98.6%
Quratulain et al. (Quratulain et al., 2010)	Texture based Features	SVM	90 MRI Scans (62 Normal, 28 Abnormal)	99.63%
Abdullah et al. (Abdullah et al., 2011)	DWT	SVM	32 Patients Dataset (10 Normal, 22 Abnormal)	65%
Zhang et al. (Yudong Zhang et al., 2011)	DWT + PCA	BPNN	66 MRI Scans (18 Normal, 48 Abnormal)	100%
Lahmiri et al. (Lahmiri, 2011)	2nd Level DWT	Ensemble based (KNN, PNN, SVM)	56 T2 MR Images (5 Normal, 51 Abnormal)	98%
Yang et al. (Yang & Fei, 2011)	Texture based Features	Multi-Scale Multi-Block FCM	21 MRI Scans	-
Zhang et al. (Yudong Zhang et al., 2011)	DWT + PCA	Bee Colony Algorithm	55 MRI scans (15 Normal, 40 Abnormal)	100%
Abdullah et al. (Abdullah et al., 2011)	DWT + PCA	SVM	32 Patients Dataset (10 Normal, 22 Abnormal)	85%
Mesrob et al. (Mesrob et al., 2012)	Region of Interest (ROI) based features	SVM	23 MRI Slices	99%

3.2   Brain MRI Segmentation

Separating an image into smaller parts is called Image Segmentation, a process used to extract useful information for image analysis. The human brain has three major types of tissues: white matter, gray matter, and cerebrospinal fluid. In MR images, it is a difficult process to recognize and separate these different brain tissue regions due to the similarity among them. Anisotropic diffusion-based brain MRI segmentation was performed by Arfan, et al. by applying 2D anisotropic diffusion filters which degrade image gradient (Jaffar et al., 2012). Further results were improved by applying the active contour model on the resultant segmented image. Quratulain et al. proposed brain MRI segmentation using fuzzy c-mean clustering (FCM) (Quratulain et al., 2010).

Nicolae Duta performed segmentation of brain MR images using active shape models (Duta & Sonka, 1998). He used the Euclidian plane to describe object contours, and then calculated brain shape statistics. He used eigenvectors on the brain structure and used edge cliques to determine edge strengths and gray level appearance. Fletcher-heath proposed automatic brain tumor segmentation based on three-step FCM clustering, and enhanced the results by integrating domain knowledge and image processing (Fletcher-Heath, Hall, Goldgof, & Murtagh, 2001). In the first step, he applied FCM and extracted integrated tissues. In the second step, he removed the necrosis by applying T1 histogram and used ventricle approximation to remove pixels within the ventricles. In the final step, he built a 3D volume and identified the tumors for the most compact and high variance regions. Meritxell, et al. performed brain segmentation in five different classes by applying statistical classification methods on T1-weighted brain MR images (Cuadra,

Cammoun, Butz, Cuisenaire, & Thiran, 2005). Different unsupervised statistical methods such as the Finite Gaussian Mixture Model (FGMM), the Gaussian Hidden Markov Random Field Model (GHMRF), the Gaussian and Partial Volume Model (GPV), and the Error Probability Minimization Model (EP) are being discussed for brain segmentation.

Table 3: Summery of Brain MRI Segmentation techniques.

Author(s)	Description	Data	Segmentation
Duta et al. (Duta & Sonka, 1998)	Segmentation by Active Shape Model	27 MR Images (8 for Training, 19 for Testing)	Brain, Brain Tissues
Fletcher et al. (Fletcher-Heath et al., 2001)	Non Enhancing Brain Tumor Segmentation	45 MRI of 6 Patients (14 of 2 Patients for training, 31 of 4 Patients for testing)	Brain Tumor
Marroquin et al. (Marroquin et al, 2002)	Segmentation by Bayesian Method	58 Simulated Images and 40 Real Brain MR Images	Brain
Cuadra et al. (Cuadra et al., 2005)	Statistical Classification of T1 Brain MRI	187 Simulated Images and 146 Real Brain MR Images	Brain Tissues
Quratulain et al. (Quratulain et al., 2010)	Segmentation using Texture Analysis	90 MRI Scans	Brain Tumor
Chen-Ping et al. (C. Yu, Ruppert, & Nguyen, 2012)	Statistical Asymmetry based Segmentation	17 MRI Slices	Brain Tumor
Arfan Jaffar et al. (Jaffar et al., 2012)	Anisotropic Diffusion based Segmentation	187 MRI Scans	Skull, Brain, Tumor

CHAPTER 4

IMAGE ANALYSIS AND BRAIN PART EXTRACTION

Brain segmentation is a very important task due to complex anatomy of the brain structure and the skull. Most brain MR scans are highly correlated with low contrast, which make segmentation more difficult. For a comprehensive study of brain MR images, we need to differentiate various patterns which can be done through segmentation of the brain from the rest of the skull part from the MRI.

Image segmentation is used to divide an image into different segments based on specific criteria so useful information can be extracted for the comprehensive analysis of an image. Brain tissue can be classified into three main types, which are White Matter (WM), Gray Matter (GM), and Cerebrospinal Fluid (CSF). Correct partitioning of these tissues is the most important task for brain image processing. The complexity and inconsistency of the brain anatomy makes the MR image segmentation more difficult. Another common issue when it comes to MR image segmentation is labeling voxels according to these three tissue types (Y. Zhang, Brady, & Smith, 2001). Correct segmentation of MRI plays a significant role in meaningful analysis because most MR images are low contrast images and brain tissue classes can easily overlap.

In this chapter, we have applied the state-of-the-art image segmentation techniques and implemented suitable steps to improve the results. For brain part extraction, we first performed our testing on simulated brain MRI data. After getting satisfactory results, we did the testing on real MRI datasets and measured the results where accuracy based on

the manually-segmented MR images. We adopted three methodologies to distinguish the brain from the rest of the MR image.

4.1 Segmentation using Boundary Detection and Region Growing

Medical image segmentation is a problem and there is no uniformly-recognized method that accurately segments medical images. Measurement-based techniques do not provide closed contours, so combined region-growing-based segmentation approaches produce better results. In images, boundary detection acquires image geometry and the clustering boundary points for the seed point. The process of image segmentation through edge detection and region growing is shown in Figure 7.

4.1.1 Segment Head

In an MR gray-scaled image, there is a lot of noise in the background and similarity with the skull and brain parts. We cannot remove image background by using manual threshold to MR image (Pietka, 1994). We used a special operator which started from the right and left corners of the image and moved towards the center of the image, and then chosen the pixel class based on the average threshold value of the input image. Morphological operations are being used to ignore the small segments and a binary image is generated. The skull images removed from the background are generated from the binary image, which is shown in Figure 8.

Input MR Image

Segment Skull/Head

Converging Square Algorithm based center of Frequency

Phase Congruency based Edge Detection

Removal of small Boundaries

Region Growing and Filling detected

Final Brain Mask
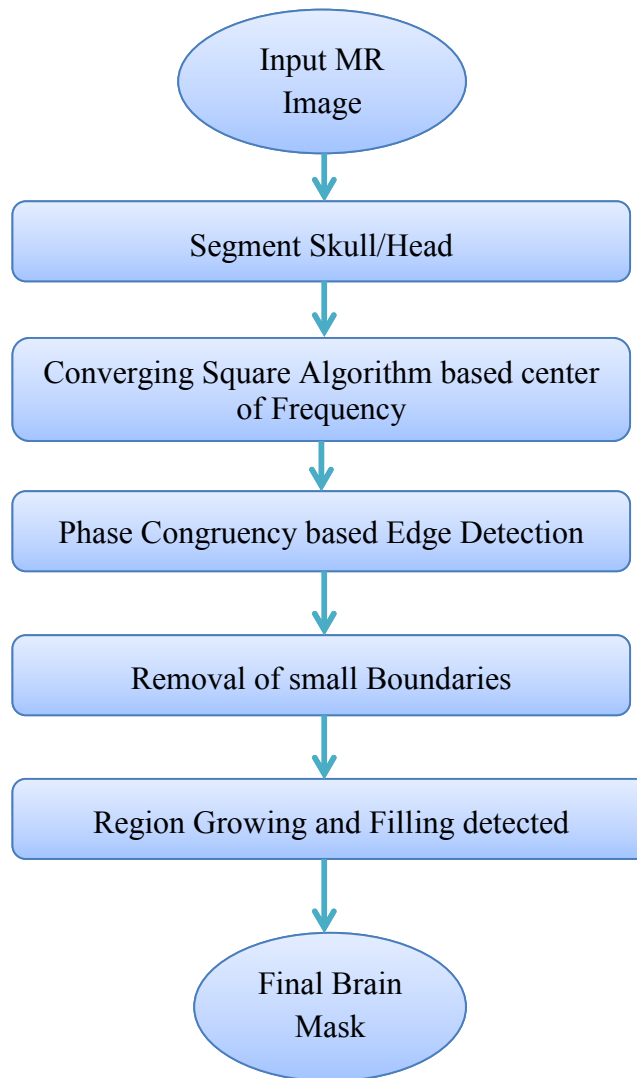
Figure 7: Flow chart of Brain MR Part segmentation using edge detection adn region growing techniques.
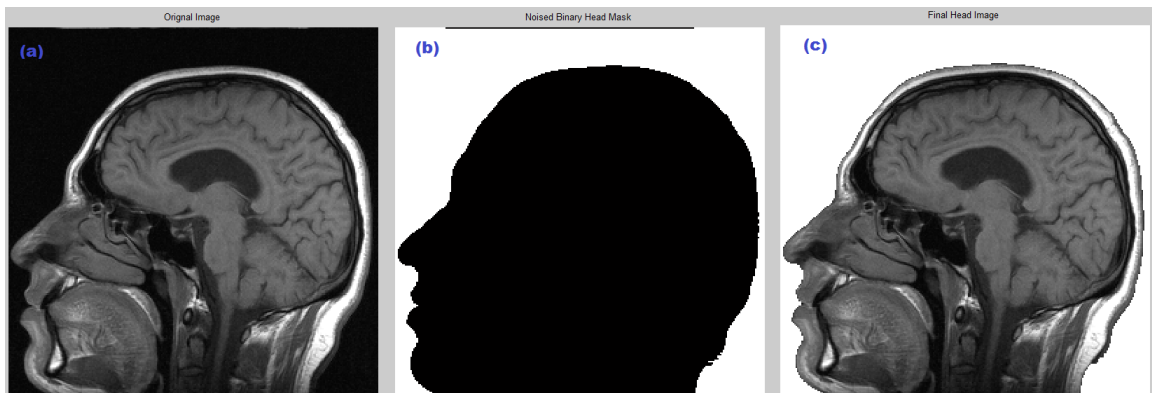
Figure 8: (a) Original MRI, (b) Noised Binary Image, (c) Skull Mask.

4.1.2 Phase Congruency based Edge Detection

Phase congruency is a low-level invariant attribute used to measure the significance of image features. The brightness and contrast of the brain MR image intensity variation with phase congruency is very fragile. It not only detects the large edges but also detects small edges in an image, along with the texture details. To extract precise edges and the phase congruency information of the image, we used Log Gabor filter with center frequency ranges from high to low. Converging square algorithm (CSA) is used to measure the Center of frequency based on the characteristics of the input image (O'Gorman & Sanderson, 1984). CSA is a method used to locate maximum density regions and their peaks in sampled two or more dimensional data. For example, an image of size k x k (in brain MRI case 256x256) is divided into four overlapping quadrangles of size (k-1) x (k-1) as shown in Figure 9. Comparison between the densities of the four quadrangles is made to choose a quadrangle with maximum density. This cycle is repeated until we reached a comparison of four pixels.
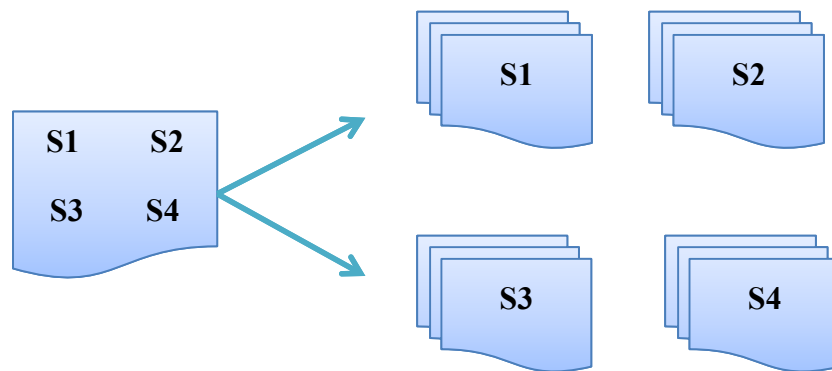
Figure 9: Dividing k×k image into 4 parts.

The edges are detected on the basis of phase congruency (PC). Kovesi defined phase congruency in Equation 4.1(Kovesi, 2000).

$$PC_2(x) = \frac{\sum_n W(x)\lfloor (A_n(x)P_n(x)-T)\rfloor}{\sum_n A_n(x)+ \varepsilon} \tag{4.1}$$

$$P_n(x) = \cos\big(\emptyset_n(x) - \emptyset(x)\big) - |\sin\big(\emptyset_n(x) - \emptyset(x)\big)| \tag{4.2}$$

Here W(x) is a weight factor for the frequency spread, epsilon ε is incorporated to avoid division by zero, $A_n(x)$ is the amplitude at location x and $\emptyset_n(x)$ is the phase angle. T is the threshold for estimating noises. The edge information is obtained based on phase congruency by Log-Gabor filters. The 2D Log-Gabor filter is constructed in the frequency domain and has the following components: the angular filter and the radial filter (Fischer, Šroubek, Perrinet, Redondo, & Cristóbal, 2007). The radial filter transfer function and angular filter transfer function are defined in Equations 4.3 and 4.4 respectively.

$$G(\omega) = \exp\left(\frac{\left(-\log\left(\frac{w}{w_0}\right)\right)^2}{2\left(\log\left(\frac{k}{w_0}\right)\right)^2}\right) \tag{4.3}$$

$$G(\theta) = \exp\left(\frac{-(\theta - \theta_0)^2}{2T(\Delta\theta)^2}\right) \tag{4.4}$$

Here w_0 represents the center frequency of the filter, k refers to the filter's bandwidth in the radial direction, θ_0 stands for the filter's orientation angle, T is a scaling factor, and $\Delta\theta$ is the orientation spacing between the filters.

To avoid broken edges, we used non-maximum suppression and adaptive dual threshold values. Non-maximum suppression is the process of marking all the pixels whose intensity is not maximal within the certain local neighborhood set as zero (Neubeck & Van Gool, 2006). This has the effect of suppressing all image information that is not part

of the local maxima. Non-maximum suppression avoids single pixel broken edges; so as to avoid offside broken edges, adaptive high and low threshold values were used.

4.1.3 Edge and Region Growing based Segmentation

Region growing is a process where initially, an arbitrary small area is selected which iteratively grows its regions based on the similarity constraints of its neighbors. In region-growing-based edges segmentation, the first step is to find out the seed pixels (Adams & Bischof, 1994). Figure 10 describes the concept of region growing.

Fan et al. introduced an automatic edge-oriented seed generation method to automate the region growing algorithm (Fan, Zeng, Body, & Hacid, 2005). The proposed method is first executed to get the simplified geometric structures of a gray level image. Centroids of the adjacent labeled edges are taken as the initial input for algorithm.

Figure 10: Example of Seed based Region Growing.

Seed pixels are obtained from the centers of the obtained clusters, while an appropriate number of clusters are obtained by using K-means clustering algorithm. K-means clustering is an unsupervised learning method used for partitioning data points into subsets of K groups (Kanungo et al., 2002). The basic idea is to outline centroids for each cluster by minimizing intra-cluster distance and maximizing inter-cluster distance. In the

next step, each data point is assigned to its closest cluster having a minimum center from its center. The algorithm aims to minimize the sum of the square error function, which is also known as objective function. The objective function for K-means is defined in Equation 4.5.

$$\text{Objective Function} = \sum_{j=1}^{k} \sum_{i=1}^{n} |x_i{}^j - \mu_j|^2 \tag{4.5}$$

Where $|x_i{}^j - \mu_j|^2$ is a distance measure between a data point $x_i{}^j$, and the cluster center μ_j is an indicator of the distance of the n data points from their respective cluster centers. Seed point based region growing flow chart is given in Figure 11.
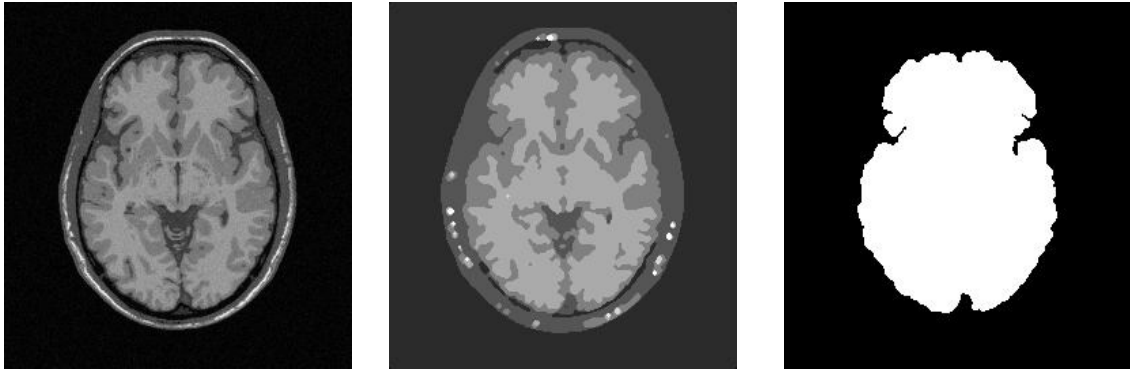
Figure 11: Output of the brain mask (a) input simulated MR Image (b) detected edges (c) region growing based segmentation.

4.2 Segmentation using Anisotropic Diffusion and Active Contours

For brain MRI segmentation using anisotropic diffusion and active contour models, we used a three-stage method to segment brain parts, which is shown in Figure 12. First of all, we removed the background noise and then generated the initial brain mask for the regions of interest. Then we refined the brain mask for a final brain mask by using active contour models.

4.2.1 Head Segmentation

In an MR gray-scaled image, there is a lot of noise in the background and similarity with the skull and brain parts. We cannot remove the image background by using manual threshold to the MR image. We used a special operator which started from the right and left corners of the image and moved towards the center of the image. It then chose the pixel, either background-or skull-based, on the gray level based on the average threshold value of the input image. Morphological operations are being used to ignore the small

30

segments, and the binary image is generated. The final skull images had been generated from the segmented binary images as shown in Figure 12. For skull boundary detection, we applied morphological operations on generated binary image which allowed us to produce an image that clearly shows the boundary of the brain.
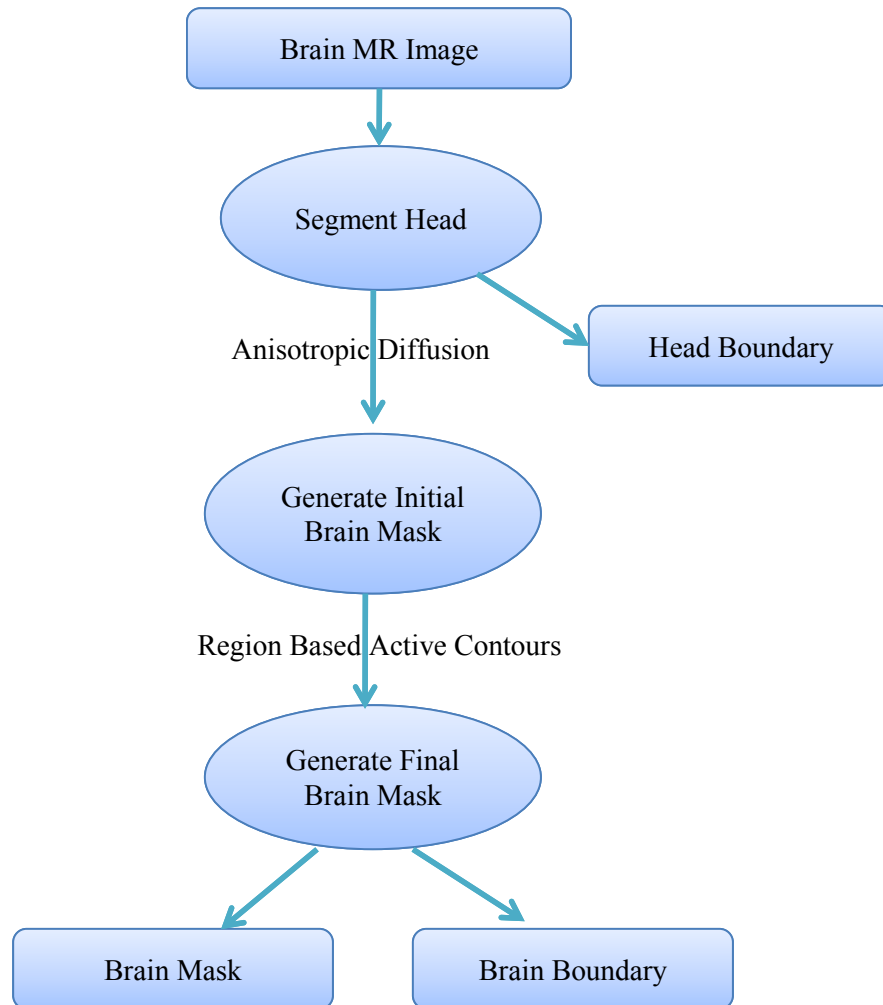
Figure 12: Process of MR segmenation based on anisotrophic diffusion and region growing.

4.2.2   Initial Brain Mask Generation

After removing the background noise, the brain mask needed to generate, which would help us to differentiate the brain parts from the whole MR image. The image is dispersed

by using the anisotropic diffusion technique on the background noise removed image of the head. Image centroid and origins of all the segments in the image helped us to remove non-brain parts and detect the brain parts only.

To make the edges of the images fuzzier and smoother, non-Linear anisotropic diffusion filter was used on the images (Y. Yu & Acton, 2002). Also, to degrade the gradient monotonically, diffusion function was applied to the image. This required updating each of the image's pixels using a number equal to the flow supplied by its four neighboring pixels. 2D anisotropic diffusion is used to offset the non-brain part. The diffused image was divided into different segments by using simple average threshold.

The anisotropic diffusion filter is a process of diffusion formulated by Perona et al. (Perona & Malik, 1990). It is used to strengthen integration smoothing simultaneously with inhabiting integration smoothing.

$$\frac{\partial}{\partial t} I(x', t) = \nabla \cdot \left(c(x', t) \nabla I(x', t) \right) \tag{4.6}$$

In the case of brain images, $I(x', t)$, x' stands for the axes (x and y) of the image, t describes how many iterations there are, and $c(x', t)$ points to the diffusion function which is represented in Equation 4.7.

$$c(x', t) = \exp\left(-\left(\frac{\nabla I(x,t)}{\sqrt{2}K} \right)^2 \right) \tag{4.7}$$

The diffusion constant, represented in the equation as K, has a value that affects the filter's behavior. In Figure 13(c), we can see the image produced after utilizing anisotropic diffusion.

Parts of the brain have been segmented using an automated threshold value; this is done by taking the histogram of the diffused image and fitting the Gaussian curve into it (Wells, Grimson, Kikinis, & Jolesz, 1996). The Gaussian filter was first applied (please refer to Figure 13(d) for the image), followed by the automatic threshold technique, which was used to convert the gray level image into a binary level image (please see Figure 13(e) for the result). Binary segments were generated using automatic threshold have holes, which were further filled using morphological operations. Figure 13(g) shows the resulting image. After all gaps and spaces were filled, the image underwent erosion, a process which cut non-brain parts, such as the eyes, out of the image. The final outcome, shown in Figure 13(f), features a distinctive image of the brain.

The non-brain parts that were separated from the image underwent spatial information to make them less dense and disappear from the image. Afterwards, we picked a center point of the brain image and used it as our reference point; from there, all areas that were considered irrelevant to the study (i.e., non-brain parts) were removed from the image, as shown in Figure 13(h) (i.e., the brain image has been isolated). The next step involved dilating the image. To do this, we subtracted the isolated brain image from the original eroded image. This resulted to an image of the brain with clear boundary as shown in Figure 13(i). As a final step, we followed the original image's boundary and mapped it before extracting the boundary on the initial brain region. The final image is shown in Figure 13(j).

4.2.3 Generate Final Brain Mask

Sometimes, the generated mask does not completely fit the original brain mask, and some brain parts fall outside the boundary. To solve this problem and enhance the results, we

used the active contour model algorithm introduced by Kass, et al. (Palo & Alto, 1988).

The extracted final brain mask is shown in Figure 14.

Figure 13: (a) Noised Removed Image, (b) Head Mask Boundary, (c) Applied Anisotropic Diffusion, (d) Applied Gaussian Filter, (e) Binary Conversion, (f) Applied Erosion, (g) Region Filled, (h) Removed non brain parts, (i) Applied Dilation, (j) Initial Brain Part.
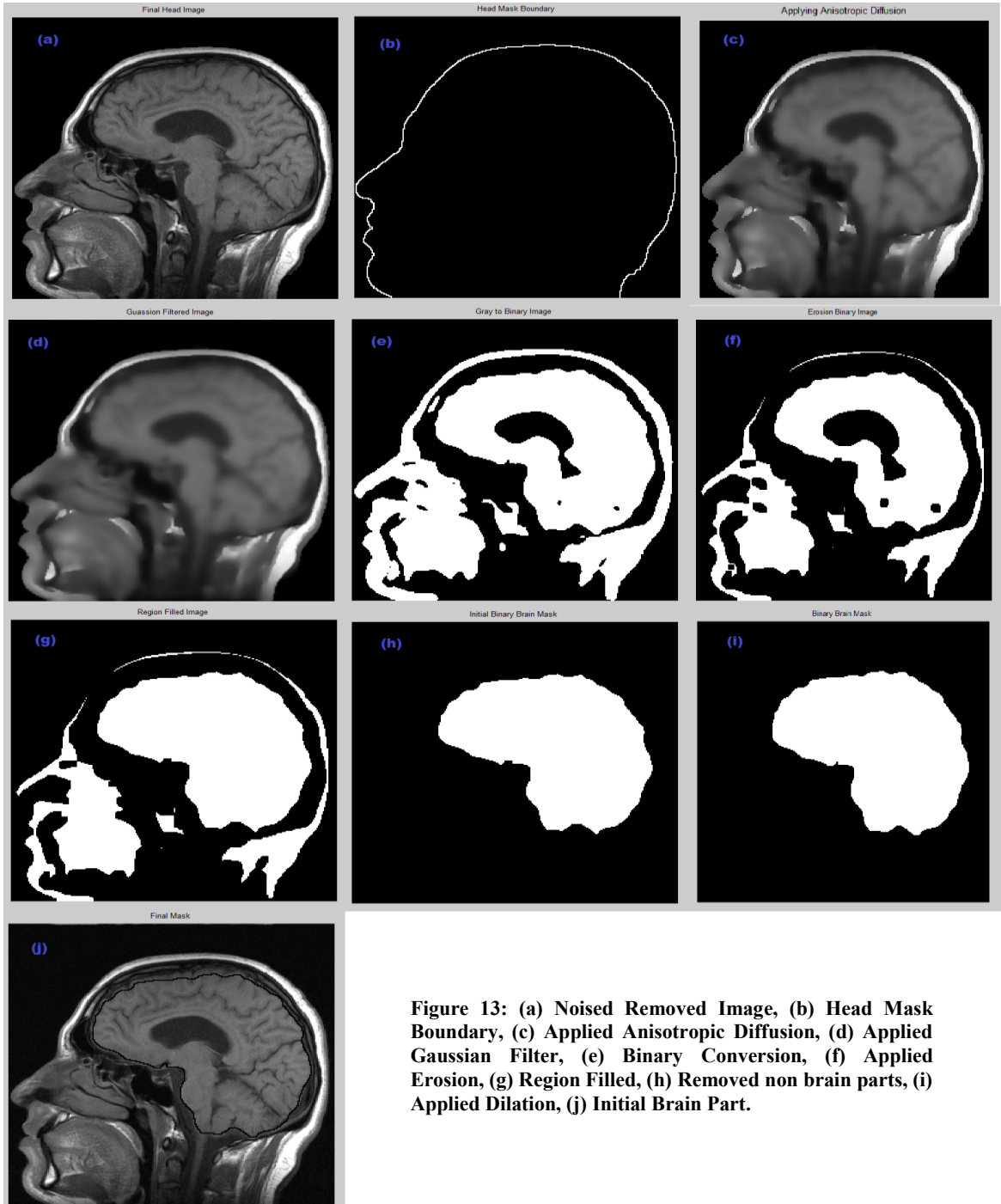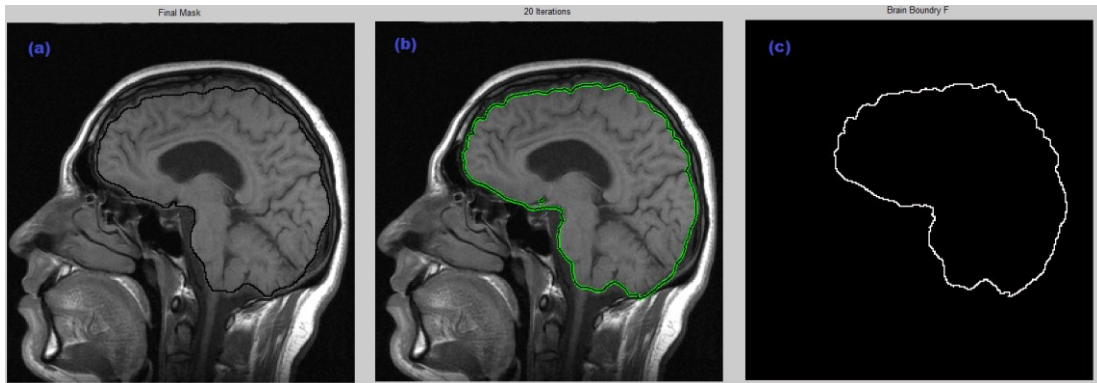
Figure 14: (a) Initial Brain Part, (b) Enhanced Brain Part, (c) Brain Part Boundary.

4.3   Segmentation using Gaussian Smoothing and Edge Detection

For brain part segmentation by using Gaussian smoothing and edge detection technique, we used 4 steps procedure. In first step we applied Gaussian low pass filter to smooth the image. In next step we binarize the smoothed image and applied morphological operations. In final step we detected the edges by using the Edge Detection by Laplacian of Gaussian and enhanced the results by using morphological operations.

4.3.1 Gaussian Smoothing

Brain MR Images contains sharp and irregular contours so image is dispersed by using Gaussian low pass filter. Low pass filter removes the high frequencies and enhances low frequencies which results the smooth MR image as shown in the Figure 15.

Original Image	Gaussian Smoothed Image
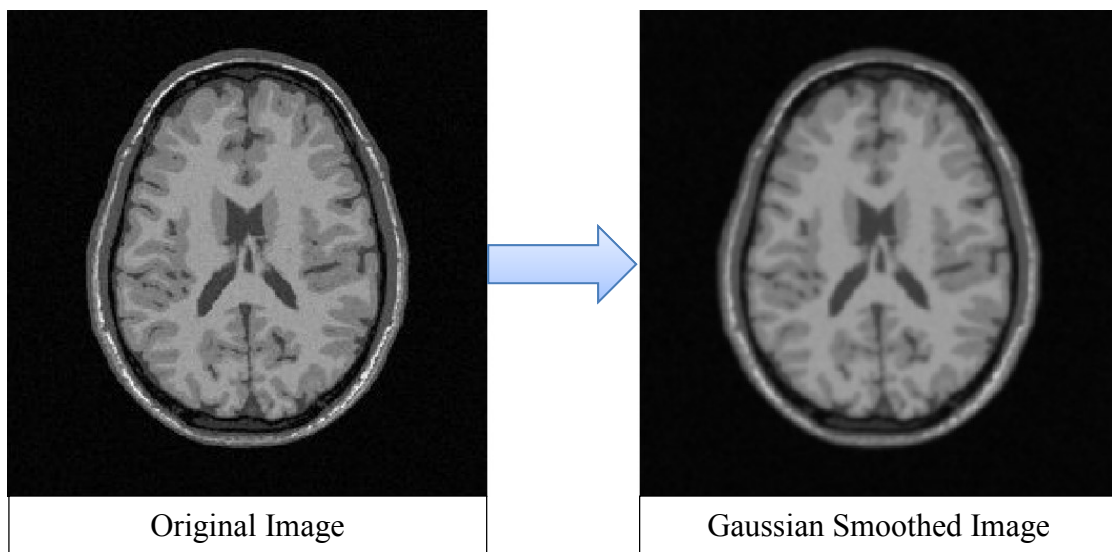
Figure 15: Gaussian Smoothed Image.

4.3.2 Binarization of the Image

After Gaussian smoothing, we converted the gray image to binary image by apply 2 way threshold. The threshold values calculated based on global image threshold using Otsu's method which chooses the threshold based on two classes of pixels to minimize the intra-class variance and maximize inter-class variance.

$$\sigma_w^2(t) = q_1(t)\,\sigma_1^2(t) + q_2(t)\,\sigma_2^2(t) \tag{4.8}$$

Where w =1, 2 are the probabilities of two classes disjointed by threshold t and σ_i variance of these classes.

$$q_1(t) = \sum_{i=1}^{t} P(i) \tag{4.9}$$

$$q_2(t) = \Sigma_{i=t+1}^{I} P(i) \tag{4.10}$$

4.3.3 Morphological Operations

Morphological operations are applied to remove the small non brain objects from the binary image. We first applied erosion on the binary image and filled the wholes. After filling the whole, applied back dilation to bring it to the original size.

4.3.4 Edge Detection by Laplacian of Gaussian

Laplacian of an image point out regions with high intensity change so it is being used for the edge detection. Laplacian L(x,y) of image with pixel intensity values I(x,y) can be represented in the form of second derivate measurement.

$$L(x, y) = \frac{\partial^2 I}{\partial x^2} + \frac{\partial^2 I}{\partial y^2} \tag{4.11}$$

Second derivate based Laplacian kernels are very sensitive to the noise. To reduce noise and improve edges detection results, image is being smoothed Gaussian filter before applying Laplacian filter which is also known as Laplacian of Gaussian (LoG). Larger value of the sigma in Gaussian filter increases the smoothing. Two dimensional Gaussian distribution is the product of two one dimensional Gaussian distribution G(x) and G(y).

$$G(x) = \frac{1}{\sqrt{2\pi}.\sigma} . e^{-\frac{x^2}{2\sigma^2}} \tag{4.12}$$

$$G(x,y) = G(x).G(y) = \left(\frac{1}{\sqrt{2\pi}.\sigma} . e^{-\frac{x^2}{2\sigma^2}}\right).\left(\frac{1}{\sqrt{2\pi}.\sigma} . e^{-\frac{x^2}{2\sigma^2}}\right) \tag{4.13}$$

$$G(x,y) = \frac{1}{2\pi\sigma^2} . e^{-\frac{x^2+y^2}{2\sigma^2}} \tag{4.14}$$

LoG equation can be formulated for the second derivate of the 2D Gaussian Function equation.

$$LoG(x, y) = -\frac{1}{\pi\sigma^4}\left[1 - \frac{x^2 - y^2}{2\sigma^2}\right]e^{-\frac{x^2+y^2}{2\sigma^2}} \qquad (4.15)$$

Where x and y are distance from the origin in horizontal and vertical axis respectively while σ is the standard deviation of the Gaussian distribution. MR image segmentation results are shown in Figure 16.

| Original MRI | Binaried MRI | Segmented MRI |
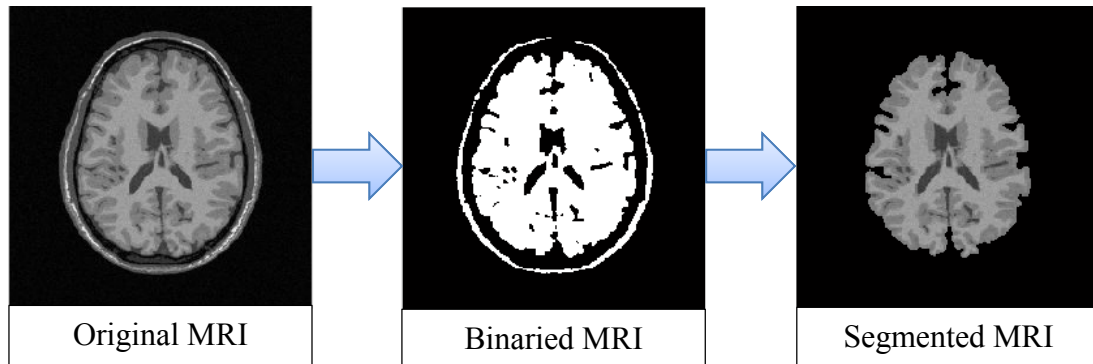
Figure 16: Segmentation by using Gaussian Filters and Edge Detection.

4.4   Performance Measures

The developed prototypes of the all three methods are evaluated on the simulated MRI datasets and the real datasets and we measure the performance by means of Receiver Operating Characteristic (ROC), Mutual Information (MI) and Dice Similarity Coefficient (DSC).

4.4.1 Receiver Operating Characteristic

ROC is used to measure the performance of the binary classifier based on the True

Positive (TP), False Positive (FP), True Negative (TN) and False Negative (FN).

Figure 17: ROC based binary classification outcome table.

Accuracy, Sensitivity and Specificity of the test is measured based on the ROC outcome

table as shown in the Equation 4.16, 4.17, 4.18.

$$Accuracy = \frac{(TP+TN)}{(P+N)} \tag{4.16}$$

$$Sensitivity = \frac{TP}{(TP+FN)} \tag{4.17}$$

$$Specificity = \frac{TN}{(FP+TN)} \tag{4.18}$$

From the ROC outcome table, we calculated different performance matrices which includes Accuracy, Sensitivity and Specificity of the simulated and real MRI datasets outcomes and compare the results.

4.4.2 Mutual Information

Mutual information is used to measure the performance of the outcome based on the joint probability distribution. It is a qualitative measure that how much a random variable correlates with the other random variable. We can measure the mutual information two class problems by considering them as random variable X, Y and by using joint probability distribution equation.

$$MI(X,Y) = \sum_{x \in X} \sum_{y \in Y} p(x,y) \times \log \left(\frac{p(x,y)}{p(x)p(y)} \right) \tag{4.19}$$

Where $p(x,y)$ is joint probability distribution of X and Y.

4.4.3 Dice Similarity Coefficient

Dice similarity coefficient is statistical method used to measure similarity in between two classes. The equation is used to measures the dice similarity coefficient of two class problem.

$$DSC(X,Y) = \frac{2|A \cap B|}{|A| + |B| + 2|A \cap B|} \tag{4.20}$$

Results of the Region growing based, anisotropic diffusion based and Laplacian of Gaussian based method are described in Table 4. Graph describes the comparison different performance measures of simulated and real dataset.

Table 4: Performance Measures of Brain Part Extraction.

Source	Simulated Dataset		Real Dataset	
	BrainWeb: Simulated Brain Database		PIMS Real Benchmarked Dataset	
# of Scans	30 MRI Scans		164 MRI Scans	
Method	RG	Anisotropic	RG	Anisotropic
Accuracy	98.31%	97.92%	96.48%	96.41%
Specificity	98.42%	98.22%	96.49%	96.36%
Sensitivity	98.37%	98.29%	96.47%	96.52%
DSC	99.22%	98.86%	98.19%	98.15%
MI	98.28%	98.25%	96.48%	96.41%

CHAPTER 5

FEATURE EXTRACTION

Feature extraction is a technique in which an image is transformed into its basic set of features. In brain tumor analysis, the first step is the classification of the image and for this purpose, useful features are extracted. It is very important to extract good features, but it is a very challenging task. There are many different methods to extract a feature from an image. Some famous methods are Gabor features, texture features, principal component analysis, feature based on wavelet transform, discriminant analysis, decision boundary feature extraction, and minimum noise fraction transform.

5.1 Feature Extraction Methods

One important task before image feature extraction is image feature selection. Selection of a feature will define the performance of the image extraction and eventually will affect the classification. By using optimum feature set, the classifier can achieve higher accuracy. One method which is given in the related literature is based on Fisher discriminant analysis extracts features using normal distribution or complex distribution. Another method uses enhanced stochastic learning, while a third method is designed for face recognition and uses multi-resolution metric and dominant frequency features. This technique improves the performance of object recognition to a great extent. Another technique uses reference images to extract the features directly by checking the similarity

among different images. In this method, the feature vector is calculated by using the correlation between the original image and the reference image, which enhances the performance.

5.2   Discrete Cosine Transform

Discrete cosine transform (DCT) is used to isolate images into parts depending upon the image visual features. The discrete cosine transform shares a similarity to the discrete Fourier transform (DFT) being used to transform images from a spatial domain to a low-frequency domain. 2D-DCT is most commonly used for image and signal processing due to its strong compaction property. One dimensional DCT of N data points is defined in Equation 5.1, where F is the linear combination of the basis vectors.

$$F(\mu) = \left(\frac{2}{N}\right)^{\frac{1}{2}} \sum_{i=0}^{N-1} A(i).\cos\left[\frac{\pi.\mu}{2.N}(2i+1)\right] f(i) \tag{5.1}$$

One dimensional DCT is applied to each row and column of F to get two dimensional DCTs. 2 dimensional discrete cosine transform of *nxm* image is defined in Equation 5.2.

$$F(\mu, v) = \left(\frac{2}{N}\right)^{\frac{1}{2}} \left(\frac{2}{M}\right)^{\frac{1}{2}} \sum_{i=0}^{N-1} \sum_{j=0}^{M-1} \Delta(i).\Delta(j).\cos\left[\frac{\pi.\mu}{2.N}(2i+1)\right] \cos\left[\frac{\pi.\mu}{2.M}(2j+1)\right].f(i,j)$$

$$\tag{5.2}$$

Where $0 \leq u \leq N$, & $0 \leq v \leq N$ while Inverse 2D DCT transform is simple F-I(u,v).

$$\Delta(\varepsilon) = \begin{cases} \frac{1}{\sqrt{2}} & for\ \varepsilon = 0 \\ 1 & otherwise \end{cases} \tag{5.3}$$

5.2.1 Brain MRI Features Extraction based on DCT

We used 2D discrete cosine transform to calculate the DCT features of the brain MR image. We applied the natural logarithm on each absolute element value of corresponding element. We calculated the two dimensional discrete cosine transform of the image by using the proposed system, which is shown in Figure 18.
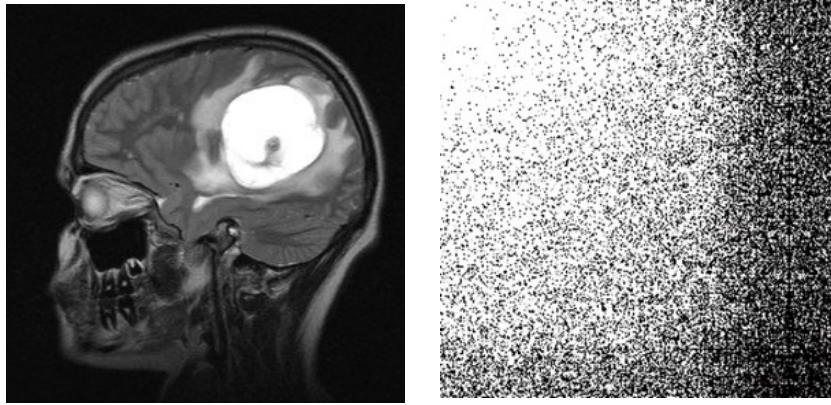
Figure 18: 2D DCT (Log abs) of the MR Image.

5.3   Discrete Fourier Transform

Discrete Fourier Transform (DFT) is a process to transform finite time based data into discretized frequency based data. The input dataset to the DFT consists to the complex and produces complex number within particular range of frequencies. The DFT is defined in equation which transformed N sized complex time domain numbers $x_0, x_1, x_2, x_3, \ldots,$ x_n into N frequency domain complex numbers.

$$X(k) = \sum_{n=0}^{N-1} x(n) e^{\frac{-i2\pi nk}{N}} \tag{5.4}$$

Fast Fourier Transform (FFT) algorithm is being used to calculate DFT and inverse DFT in an efficient way. Magnitude of the DFT computed complex numbers is being computed by using the real and imaginary parts.

$$A = \sqrt{R^2 + I^2} \tag{5.5}$$

where A is the absolute magnitude value of the real part R and imaginary part I of the complex number.

5.3.1   Brain MRI Features Extraction based on DFT

We used 2D fast Fourier transform to calculate the DFT features of the brain MR image. We rearranged the DFT output by moving the zero frequency component to the center of the array. We applied the natural logarithm on each absolute element value of corresponding element. We calculated the two dimensional discrete Fourier transform of the image by using the proposed system, which is shown in Figure 19.
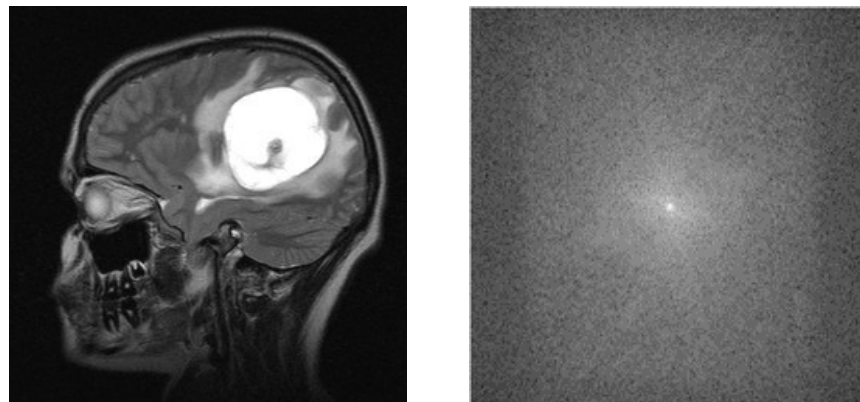

Figure 19: 2D FFT of MR Image.

5.4   Discrete Wavelet Transform

Through wavelet transform, a signal can decompose into some basic functions, which are called wavelets. A wavelet is used in image processing as a multi-resolution technique to analyze an image's texture. For purposes of classification, wavelet coefficients are utilized as features vector. One technique used for extracting features is the Discrete Wavelet Transform. DWT is considered to be more efficient and less expensive in terms of computation (Sun, Dong, & Xu, 2006). As such, our proposed system used discrete wavelet transform the extract an image's features.

Continuous wavelet transform (CWT), on the other hand, is an extension of DWT which uses basic mother wavelet. CWT is a version of the mother wavelet transform that is shifted and scaled. CWT in relation to real valued wavelet, $\psi(x)$ for continuous, square-integrable function f(x), is defined as:

$$W_\psi(p,q) = \int_{-\infty}^{\infty} f(x)\psi_{p,q}(x)dx \qquad\qquad (5.6)$$

$$\psi_{p,q}(x) = 1/\sqrt{p}\; \psi(\tfrac{x-q}{p}) \qquad\qquad (5.7)$$

Where p is a scaled parameter and q is a translation parameter (R.C. Gonzalez, 2008).

As a function of linear transformation, an image's data undergoes DWT and breaks it down, resulting to frequencies. These detailed frequency components have been shown to be in-depth calculated components.

These components are comprised of an image's horizontal, diagonal, and vertical sub-bands. A high pass filter is applied to the image, followed by a low pass filter, in order to

arrive at these components. The equations below illustrate how these components are obtained.

$$a_{j+1}[p] = \sum_{n=-\infty}^{+\infty} l[n-2p]a_j[n] \qquad (5.8)$$

$$d_{j+1}[p] = \sum_{n=-\infty}^{+\infty} h[n-2p]a_j[n] \qquad (5.9)$$

Where aj, is the wavelet function's approximation coefficient and dj is its detail coefficient. The l[n-2p] function represents the low pass filter coefficient while h[n-2p] is a function that pertains to the high pass filter. Four sub-bands – HH, HL, LL, and LH – are derived from an image after DWT is applied to it. HH, LH, and HL all represent detail coefficients, while LL stands for approximate coefficients.

5.4.1   Brain MRI Features Extraction based on DWT

We extracted brain MRI features by using level 3 discrete wavelet transform. Figure 19 show the process of 3 level discrete wavelet transform approximation and details coefficients.
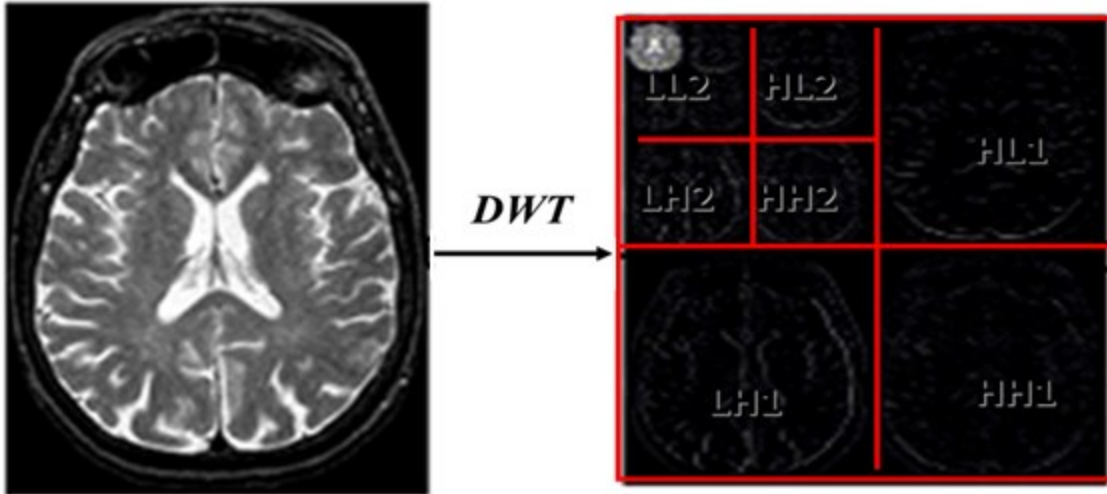
Figure 20: DWT Schematically.

5.5   Principal Component Analysis

One of the most common forms of dimensionality reduction is principal components analysis. PCA find the linear lower-dimensional representation of the data. The main idea behind using PCA in this approach is to reduce the dimensionality of the wavelet coefficients. This leads to more efficient and accurate classifier. As there is 300 to 400 images for each patient and we have to analyze most of them. Thus by extracting useful information from image we can make our system fast (Daniel X. Le, George R. Thoma, 1995).

In PCA, data points are represented as vectors in multidimensional space and projection of vector x onto an axis u is $u.x$. Direction of greatest variability calculated based on average square of the projection is having greatest i.e. u such that over all x is maximized which are illustrated in Figure 21. This direction of u is the direction of the first Principal and similarly next components are calculated.
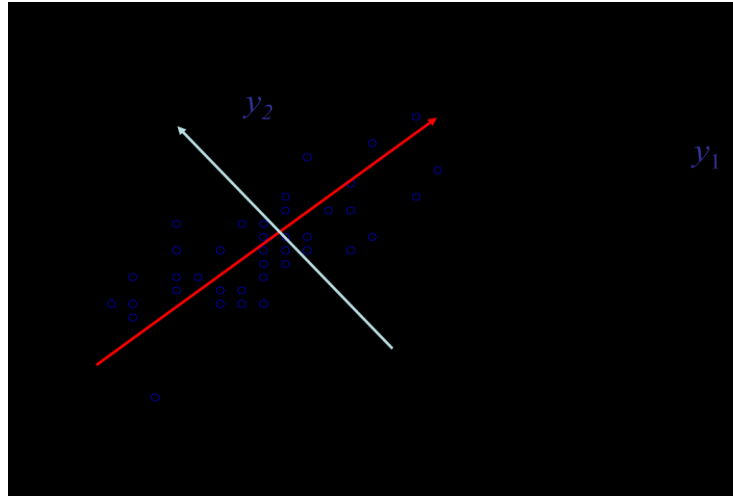
Figure 21: Interpretation of PCA.

We applied PCA on the extracted DWT frequency components which convert them into linear lower dimensions.
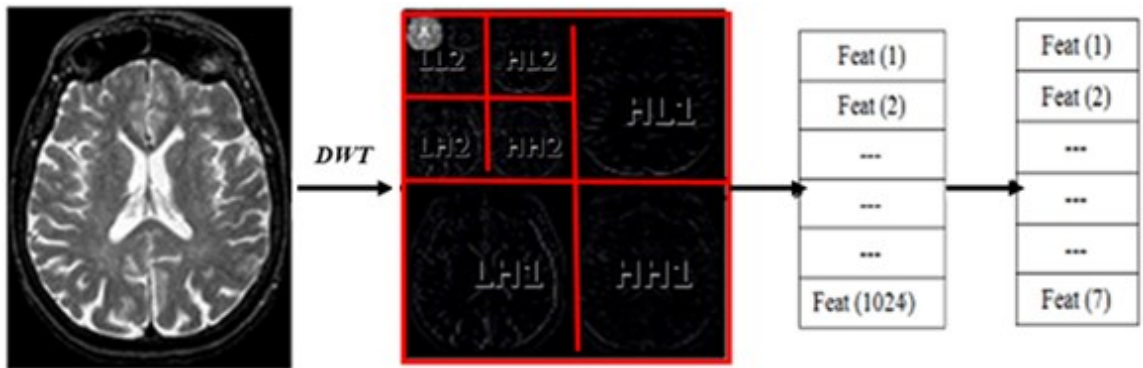
Figure 22: Schematic diagram for the PCA based features reduction.

CHAPTER 6

CLASSIFICATION AND TUMOR SEGMENTATION

Classification entails identifying input patterns and transforming them into corresponding classes. Image classification is being performed on the extracted features of the images. Classification process normally consists to three phases; training phase, validation phase and testing phase. In training phase, the models are trained based on the input features and the target values. In validation phase, the trained model is being tested to estimate best model parameters. In testing phase, test data is being applied to classify it.

Many factors need to be considered when selecting a suitable classifier. These factors include:

- ✓ Accuracy of the classification
- ✓ Performance of the algorithms
- ✓ Computational resources

Classification can be grouped into the supervised classification and the unsupervised classification (Lu & Weng, 2007). For this type of classification, the following are its most common traits:

- ✓ It does not require prior extensive knowledge of the region
- ✓ There is less opportunity for errors to happen since many detailed decisions under supervised classification are not strictly required to unsupervised classification.

✓ In order for distinct units to be identified as unique classes, they must undergo unsupervised classification.

Overall, supervised classification involves using known samples to classify unknown samples (Maria-Luiza Antonie, Osmar R. Zaıane, 2006). On the other hand, the following characteristics describe supervised classification:

✓ Extensive knowledge of the area is required.

✓ Labels also include input patters

✓ A close examination of the training data allows for the detection of possible errors and their classification, as well as proper classification.

In this chapter, we address the classification techniques used to classify brain MR images into malignant or benign.

6.1 Classification Techniques

6.1.1 Support Vector Machine

A supervised learning method and efficient classification algorithm used extensively in regression analysis and classification is the support vector machine or SVM, which operates by analyzing data and deriving trends. SVM uses kernel techniques to transform non-linearly separable data into higher-dimensional space. Its special capability, called structural error minimization, makes SVM useful and well-known across fields. It also takes a margin and computes it in order to separate classes maximally in the space.

As a classification approach, the Support Vector Machine uses hyper planes as basis (hyper planes act as segregators when it comes to common binary classification). SVM is also founded on the principle of minimizing structural errors. This allows SVM to be more accurate in predicting properly-selected parameters compared to other algorithms used for statistical classification, such as Linear Discriminant Analysis and KNN.

In Figure 19, the margin is shown, as well as the hyper plane. In the following equation, n stands for the classes' training data $\{(x1,y1), (x2,y2),\ldots, (xn,yn)\}$, $i = 1, 2, 3, \ldots\ldots, n$ in which , w stands for weight vector, b stands for bias weight, and $x_i \in R_n$ is an n dimensional space and yi $=\pm1$. With this in mind, the first two equations now show how the hyperplane can be divided into two. This separation can be described as a linear separation, while the last equation defines the hyperplane.

$$(w \cdot x_i + b) > 1 \quad if \ y_i = 1 \tag{6.1}$$

$$(w \cdot x_i + b) < 1 \quad if \ y_i = -1 \tag{6.2}$$

$$(w \cdot x_i + b) = 0 \ else \ case \tag{6.3}$$

Minimizing ||w|| has been shown to increase the gap between these two classes – something that SVM aims to accomplish. Training points x_i can be properly identified using quadratic optimization algorithms, with non-zero Lagrangian multipliers α_i acting as support vectors. The equation below best illustrates this optimization issue.

$$L_d = \sum_{i=1}^{n} \alpha_i - \frac{1}{2} \sum_{i=1}^{n} \sum_{j=1}^{n} \alpha_i \alpha_j y_i y_j x_i x_j \tag{6.4}$$

To determine decision functions, these vectors are used and the rest of the data are discarded. Since in the real world, not everything is linear, we decided to use non-linear

classification – a technique that SVM also does to separate the classes. SVM does this by adding a penalty parameter, C. A slack variable represents the frequency of errors made in classification. In the above-mentioned variables, the penalty parameter is applied on all instances in which an error occurs in the margin between classes.
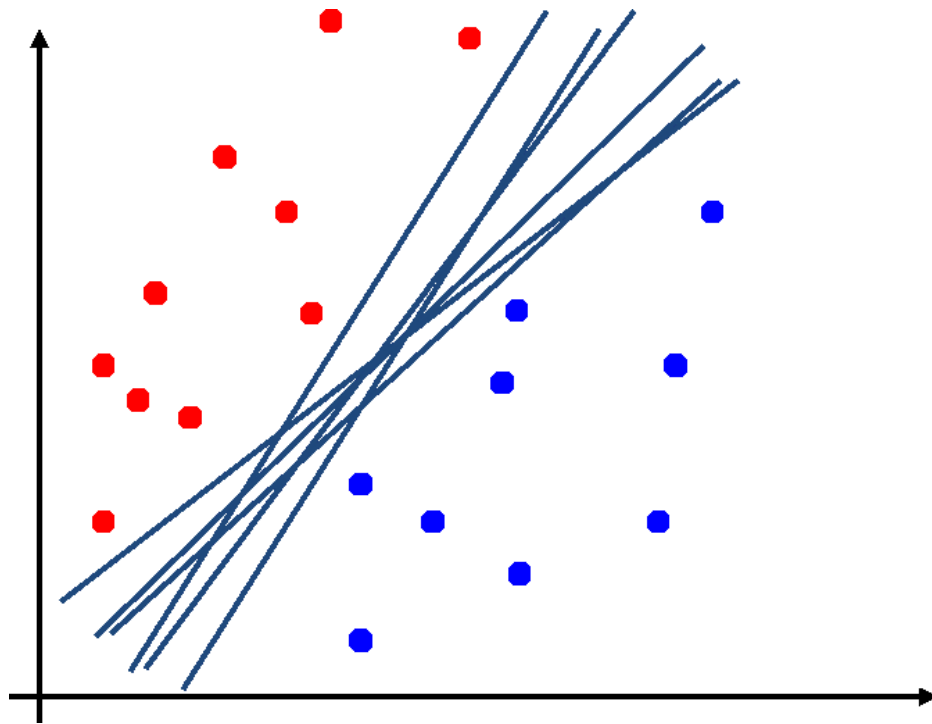
Figure 23: Support Vector Machine (Finding the optimal Line Separator).

6.1.2 Artificial Neural Network

A simulation of the human biological system, the artificial neural network (ANN) is a system based on how our biological neural networks operate. In 1943, this neural system was successfully replicated by neurophysiologist Warren McCulloch and logician Walter Pits when they introduced to the world the first artificial neuron.

A neural network can absorb and analyze information in a manner similar to how experts gain their expertise. This is because neural networks can analyze and identify patterns and trends from complex data, including ones that are incomplete, imprecise, or too complicated for humans and some basic computers to understand. Using neural networks has its benefits, including the following:

- ✓ Adaptive learning: Even with only minimal initial experience or training, neural networks can learn tasks based on the data given.

- ✓ Self-Organization: During the learning phase, the ANN can organize and represent its own information.

- ✓ Real Time Operation: Hardware devices are now being designed and manufactured specifically to capitalize on the ANN's capacity to conduct parallel computations.

- ✓ Fault Tolerance via Redundant Information Coding: Network performance degrades due to partial damage to the network. However, even with major damage to the network, some network capabilities can still be accessed and used.

The ANN is made up of layers of neuron. These neurons are assigned with weights, and then receive input and, after the activation function of the weighted sum has been determined, they produce an output. The weighted sum can be computed as the total product of an incoming input, including extra associated weight, into the overall sum.

Sometimes the network contains hidden layers; these are internal layers with neurons. The ANN's last layer can also contain neurons, either single or multiple, and this layer is

known as the output layer. When the output layer contains multiple neurons, the ANN implements multiple classifications, while single neuron in the output layer requires a simple binary classification (Haykin, 1999).

A feed forward back propagation artificial neural network (FP-ANN) has three minimum layers and is utilized as a supervised classifier (see Figure 18). The network's first layer contains input neurons, followed by the hidden layer, so-called because of the hidden neurons that form this layer in the network. Some programs contain more than one of these hidden layers. The last layer, on the other hand, contains the output neuron. Those who would handle classification are required by the FP-ANN to train before doing any classification work. This training has three stages: first, the training input pattern is fed forward. Second, the error that was identified will undergo back propagation and calculation. In the third stage, the weights are adjusted in order to minimize errors in classification. The network will only be suitable for testing after the network has been trained for this purpose (Fausett, 1994).
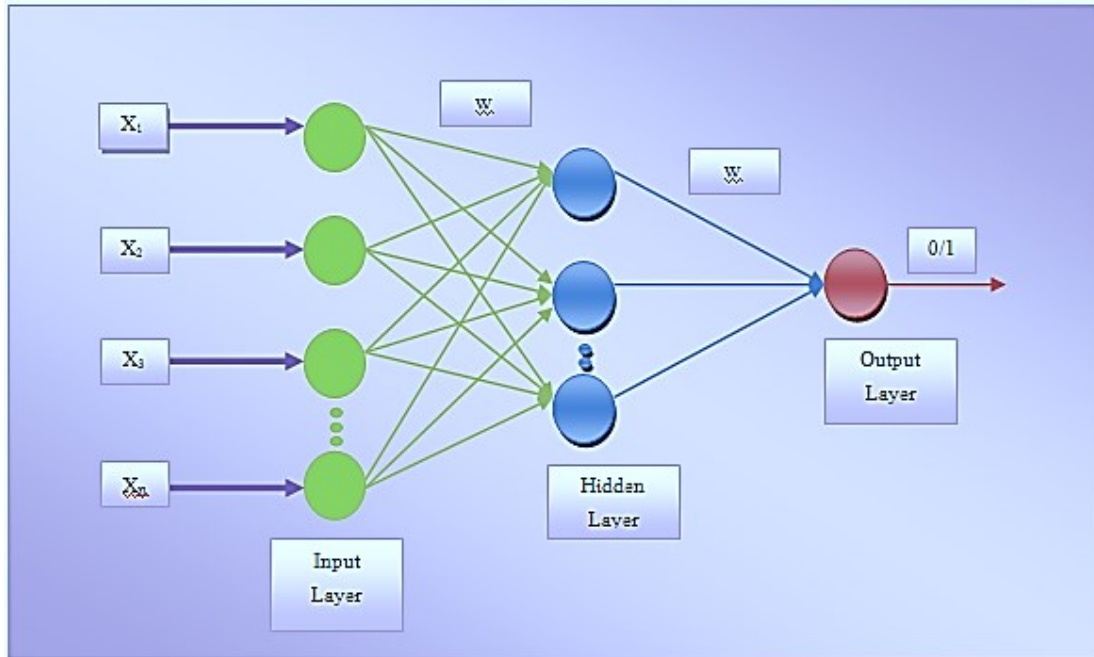
Figure 24: Architecture of the FP-ANN.

6.1.3 Bayesian Classifier

One method to compute for the features' conditional probabilities is Baye's Theory, a mathematical calculation that follows these processes (Tom M. Mitchell, 1997).

- ✓ Let X be a data sample/Object.

- ✓ Let H be some hypothesis.

- ✓ P(H) is the prior probability, which calculates the chances that a data sample is part of a specific class.

- ✓ The chances that H will be proven when compared against the observed data sample is symbolized here as P(X|H).

56

✓ The posterior probability, P(H|X), is based on data that is larger compared to the initial probability P(H), independent of X.

The equation below shows a way to calculate the posterior probability using Baye's Theorem.

$$P(H|X) = \frac{P(X|H)P(H)}{P(X)}$$ (6.5)

P(X|H) is the posterior probability of X conditioned on H. P(X) is the prior probability of X. To achieve higher accuracy, the class density estimate must also be accurate (R.O. Duda, P.E. Hart, 2001). Accuracy is dependent on the classifier, and is very dependent on class density estimates or posterior probabilities.

6.1.4 K-Nearest Neighbor

Another type of classifier is the K-nearest neighbor which is characterized by being instance-based learning and supervised classifier. New instance queries result to the classification of the majority of K-nearest neighbor category. It uses training samples and attributes to classify a new object, and it then determines which are the nearest neighbors of any instance through 'correlation' 'cosine', 'hamming', 'city block distance', or 'Euclidean' distance. The K-nearest neighbor does this on a 'random', 'nearest', or 'consensus' rule, with ties broken randomly (T. Mitchell, 1997).

What makes K-nearest neighbor important is that since its process of classification involves analyzing a small group of objects that are similar, it is found to be very useful for multi-modal classes wherein several objects with independent variables possess varying characteristics on various subsets. It has a record of being accurate even when

targeting a class that is multi-modal. On the other hand, this ability to quickly compute for similarities means the K-nearest neighbor treats all features as equal when it computes for similarities. This leads to classification errors and poor measures of similarity, especially when it involves only a small subset of features for classification. It is illustrated in Figure 20 where instance for black-colored objects ω=3 results to grouping together the black-colored objects with red-colored objects and classifying them as belonging into the same class.
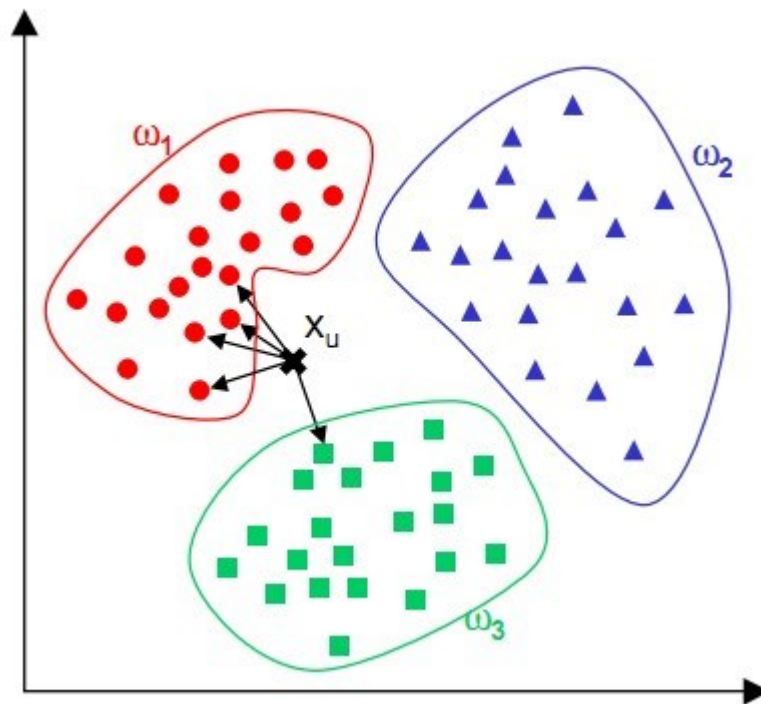
Figure 25: K-Nearest Neighbor ω=3.

6.2　　　Experimental Results for Classification

For classification, we performed several experiments on the acquired datasets from both online resources and from the medical hospitals. Performance of each classifier is measured by calculating accuracy from the confusion matrix by using unprocessed MRI images and by using the only brain part extracted MR images as input.

Table 1 describes summery of the results of comparison of the classification performance by using purposed method along with the other recent work. We applied different classification methods with different number of features along with the different experimental and testing percentage of the data distributions. We used 128 MR images dataset for the classification of normal and tumorous images. Out of 128 MR images, 44 images are tumorous and 84 images are normal. We perform tests with 5, 7, 10, 15 and 25 features dataset of DCT, DWT, DWT+PCA, DFT and calculated the average of the overall results.

We used different distribution of training, validation and testing percentages for the feature sets. We used 70% versus 30%, 50% versus 50% and 66% versus 34% for training and testing respectively. Based on the computational power required for the experiments and the performance measures, we finalized that 70% for training and 30% for testing is most suitable for the classification. Table 5 describes the performance comparison of the different classifiers along with the different feature sets. The results shows that we achieved significant increment in performance by using brain part extracted MR images features as compared to the normal MR images features.

Table 5: Comparison of different classification methods along with different type of MR image features.

Features/Classification Methods	Normal Real Data (Accuracy %)	Brain Part Extracted Data (Accuracy %)
SVM + DCT	81.58%	94.73%
SVM + DWT	92.18%	93.75%
SVM + DWT + PCA	71.05%	86.84%
SVM + DFT	67.19%	67.18%
Naïve Bayes + DCT	87.50%	82.81%
Naïve Bayes + DWT	87.50%	89.06%
Naïve Bayes + DWT + PCA	73.68%	94.74%
Naïve Bayes + DFT	42.16%	70.31%
KNN + DCT	97.37%	100%
KNN + DWT	93.75%	100%
KNN + DWT + PCA	86.84%	96.87%
KNN + DFT	68.42%	65.62%
MLP + DCT	92.10%	92.10%
MLP + DWT	93.75%	100%
MLP + DWT + PCA	81.58%	95.31%
MLP + DFT	67.19%	67.19%

We measured the accuracy based on the confusion matrix and also measured the TP Rate, FP Rate, Precision and Recall. Figure 25 describes the graph of performance for SVM classifier for both normal MR images and brain part extracted MR images by using

different feature sets. The results shows that we got better results with brain part extracted features as compare to the normal MR images.
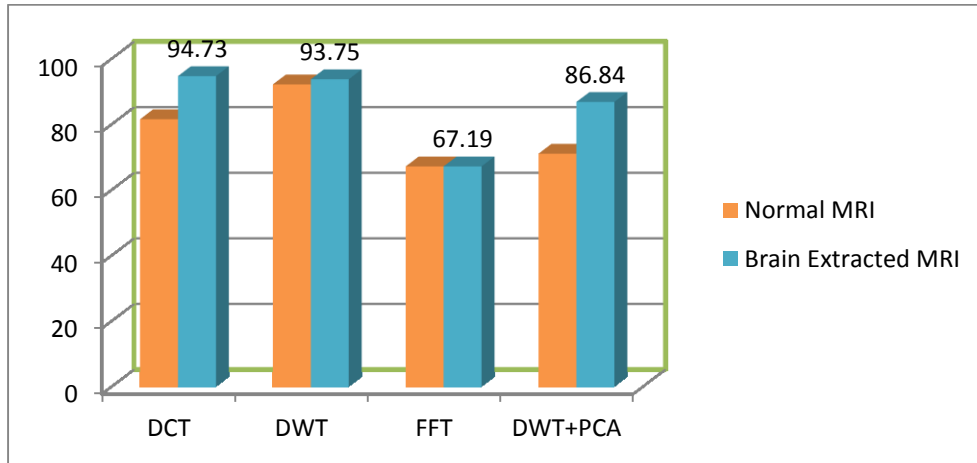
Figure 26: Graph of SVM performance for different feature sets.

We tested our proposed method on Naïve Bayes classifier which is based on the Bayes algorithm. Figure 26 describes the graph of Naïve Bayes classifier with different feature sets. The graph shows that we achieved best results by using brain part extracted DWT and PCA features.
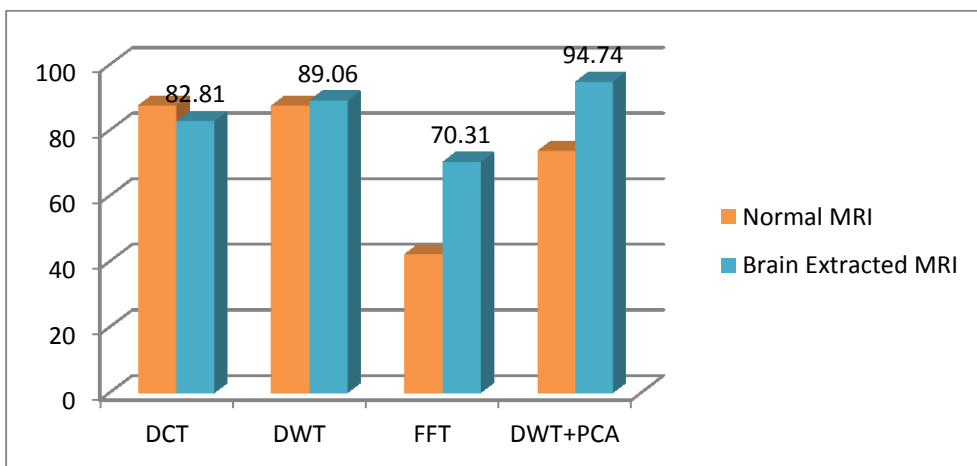
Figure 27: Naïve Bayes performance measure for different feature sets.

Figure 27 describes the graph of the Multilayer Perceptron performance by using different feature set. The results shows that brain extracted MR image features produce better results as compared to the normal MRI images.
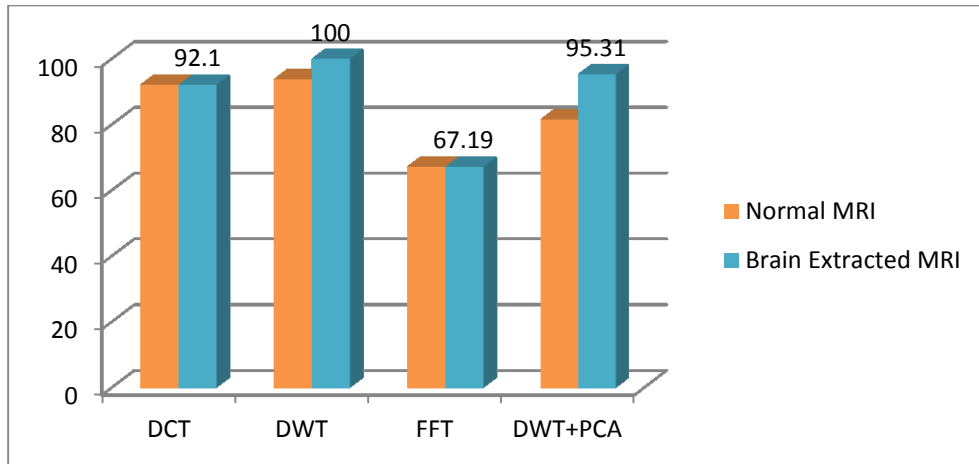
Figure 28: Graph of MLP performance for different feature sets.

Figure 28 shows the comparison graph of the KNN classifier along with the different feature sets. KNN classification result shows that achieved better results when we used features of the only brain part in the MR image as compared to the complete MR images.
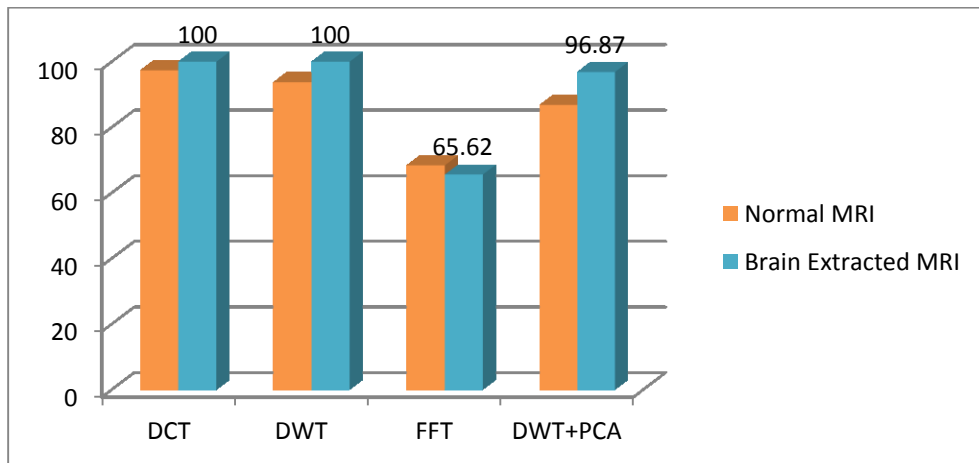
Figure 29: Graph of KNN performance for different feature sets.

Figure 29 show the comparison of all our selected classifiers along with different feature vectors. Results show that we achieved maximum performance by using features extracted from the background and skull removed image. The graph shows that KNN classifier with DCT features and MLP classifier with DWT features produces 100% accuracy rates.
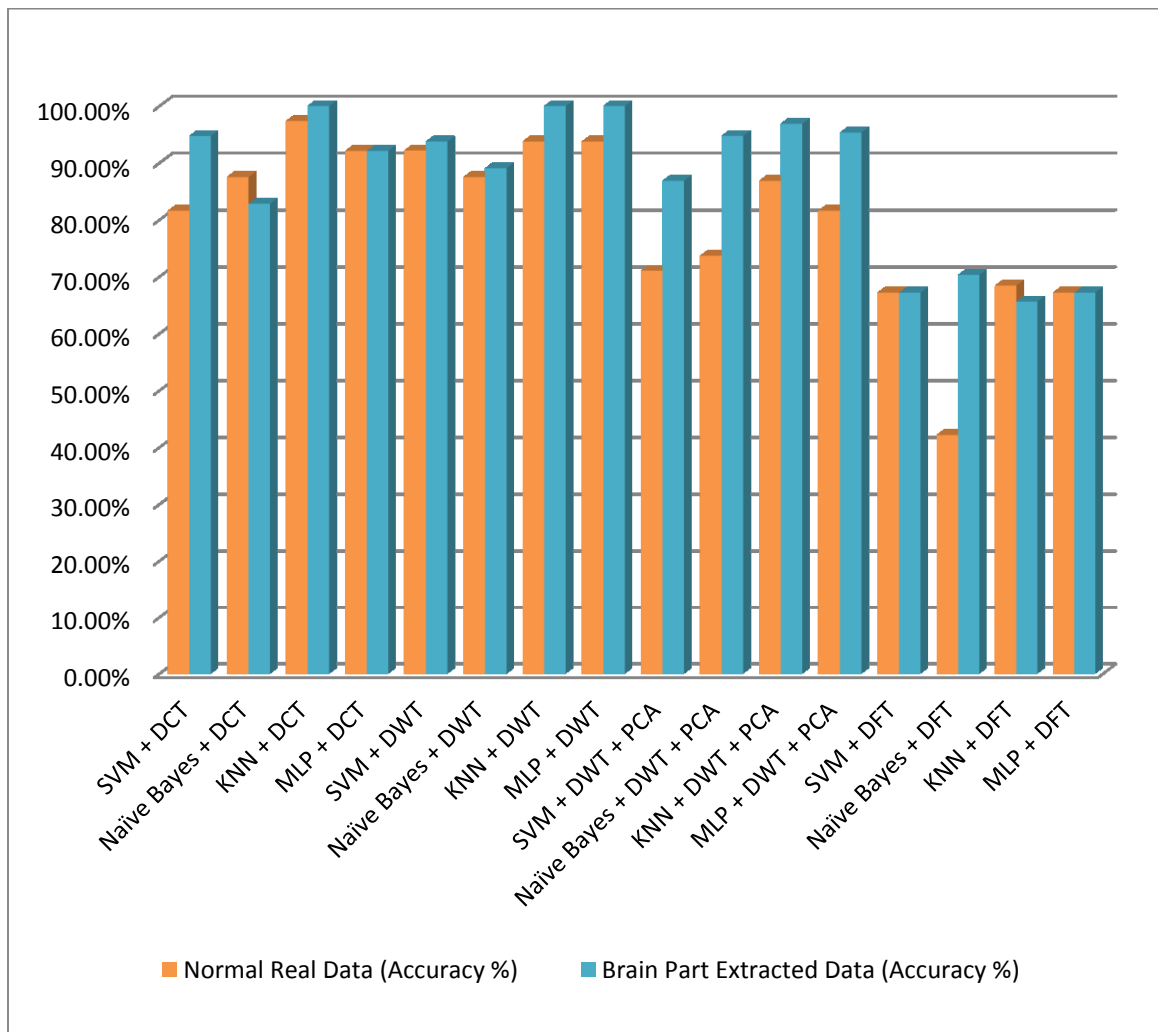
Figure 30: Comparison of different classifier performance.

CHAPTER 7

CONCLUSION AND FUTURE WORK

This chapter summarizes our major contributions in this thesis. The goal of this research is to analyze brain tumors and classification of brain MR images. This chapter also discusses the limitations of our work with possible enhancements and future research directions.

7.1   Conclusion

In this thesis we picked up one of the most complicated death causing issue. We tried to enhance results for accurate skull, brain and tumor segmentation, and brain MRI classification by using machine learning techniques. Manual classification and detection of tumors is time consuming task and there are a fewer number of radiologist for proper interpretation of Brain MR Images especially in under developed countries.

Brain segmentation is a very important task due to the complex anatomy of the brain structure and the skull. Most brain MR scans are highly correlated with low contrast, which make segmentation more difficult. Background noise is removed by using special operator which starts from the right and left corners of the image and moved towards the center of the image and choose the pixel belongings based on the threshold value. For brain part extraction, we first performed our testing on simulated brain MRI data and after getting satisfactory results, we did the testing on real MRI datasets. We applied

three different image segmentation techniques on brain MR images and segmented skull and brain parts from the MR images. The results show that we achieved high accuracy by using phase congruency based edge detection and region growing method.

We extracted features and applied different classification techniques on both unprocessed brain MR image and brain part extracted image for classification of normal and abnormal images. The experimental result shows that our proposed method got high accuracy on all type of features and all classifier along with different feature sets of brain part extracted MR image.

7.2 Future Work

In this dissertation we segmented skull, brain from the MR image and classified the brain MR image into benign and malignant. We provided first step towards the fully computer aided device for the brain tumor detection and visualization. In future, further we can improve the system by finding out the tumor location, size and growth rate which will help to the radiologist.

In future, we can measure the size and location of tumor in the brain which will be helpful for the neurosurgeons for analysis and detecting the tumor from MRI scans. They can check the position, size and type of the tumor and make decisions which will help to give suggestions about treatment and further tests for patient.

In computer graphics, 3D modeling is the process of developing a mathematical representation of any three dimensional object via specialized software and programming languages. The final product is called a 3D model. It can be displayed as a two-

dimensional image through a process called 3D rendering or used in a computer simulation of physical phenomena.

Today, 3D models are used in a wide variety of fields. For example, the movie industries use them as characters and objects for animated and real-life motion pictures. The video game industry uses them as assets for computer and video games. The science sectors use them as highly detailed models of chemical compounds. 3D modeling is also used in medical science for detailed models of organs.

Due to the importance of 3D modeling we can make the brain 3D model which help to analyze the patient tumor detected through the segmentation of MRI scans. The extracted boundaries of the skull, brain and tumor can be used to construct 3D model.

Clinical decision support systems help the medical experts in making decisions to diagnose the diseases. Semantic web plays an important role in decision making. So it can also be used in brain tumor treatment decision making. Semantic Web Technologies (SWT) is gathering more and more attention within the sphere of clinical decision support.

APPENDIX A

WORLD HEALTH ORGANIZATON BRAIN TUMOR

CLASSIFICATION

More than 120 types of brain tumors have been discovered. Today, World Health Organization (WHO) brain tumor classification system is being adopted by most of the medical institutions (Kleihues & Sobin, 2000). Tumor classification and level of tumor helps to predict its likely behavior like its growth rate and effects on the subject. There are number of ways to classify the brain tumor but following three methods of classification are more common.

I. Classification on the Basis of Brain Cells Behavior

The WHO classifies brain tumors in to two classes on the basis of cell origin and how the cells behave.

a. Benign Brain Tumors

Benign tumors remain separate from the brain primary cells and these tumors are less serious but these tumors still cause serious problems in brain when they grow. These tumors do not consist of cancer cells. The borders of benign tumors are easily identifiable and are possible to remove without effecting brain cells (Gerhardt, W., J. Clausen, E. Christensen, 1967). Benign tumor cells do not spread easily to other parts of brain but still there is a chance that a benign brain tumor may become malignant.

b. Malignant Brain Tumors

Malignant brain tumors which affect to the primary brain cells and become cause of brain cancer. This type of brain tumors grow very quickly and damage primary brain cells. Malignant tumors are more severe and death causing as compared to benign tumors. Sometimes malignant tumors spread to other parts of the brain like spinal cord and also damage its cells.

II. Classification on the Basis of Brain Cells Behavior

Brain tumors are divided to different grades from low to high based on tumors type and its effects. These grades of an individual tumor help predict its likely behavior. Brain tumors are grouped in to four grades on the basis of Astrocytoma.

- ✓ Grade-I   Pilocytic
- ✓ Grade-II   Low Grade
- ✓ Grade-III Anaplastic
- ✓ Grade-IV Glioblastoma

III. Classification based on Tumor Categories

a. Primary brain Tumors

Brain tumors that take place in brain tissue are known as primary brain tumor. These tumor cells can directly damage brain cells and become cause of death (Knopp et al., 2004).

b. Secondary brain Tumors

The brain tumor with same grade and same type of abnormal cells but are shifted from its central position to some other part of the body then it is said to be secondary brain tumor. Secondary brain tumor is different from primary as it spread to other part of the body. Doctors call secondary brain tumor as metastatic tumor. Secondary tumor is found in large quantity as compared to primary brain tumor.

APPENDIX B

METHODS FOR TUMOR TREATMENT

I. Surgery

The most usual method for treatment is surgery but before doing surgery there are some operations that should be performed. Patients with age more than 40 years should have their X-Rays and ECG tests. The process craniotomy in which surgeon open the skull and remove the tumor from the brain. Surgery is basically for the removal of tumor.

II. Radiation Therapy

It uses energy rays to destroy brain tumorous cells and also known as radio therapy. It is used to remove hidden tumor of the brain that are left sometimes during surgery or not possible in surgery. Radio therapy involves particular process patient have to visit doctor daily basis for a specific period of time. The period depends on the type, size and age of the patient.

III. Chemotherapy

The process in which drugs are used to kill tumor cells is called chemotherapy. The drugs are normally given in different rounds based on recovery period and treatment period. Chemotherapy is used for children for the delay of radiotherapy (Ausman, James I., Victor A. Levin, Willis E. Brown, David P. Rall, 1977).

References

Abdullah, N., Chuen, L. W., Kalthum, U., Khairul, N., & Ahmad, A. (2011). Improvement of MRI Brain Classification using Principal Component Analysis. *IEEE International Conference on Control System, Computing and Engineering*, 557–561.

Adams, R., & Bischof, L. (1994). Seeded region growing. *IEEE Transactions on Pattern Analysis and Machine Intelligence*, *16*(6), 641–647. doi:10.1109/34.295913

Ausman, James I., Victor A. Levin, Willis E. Brown, David P. Rall, and J. D. F. (1977). Brain-tumor chemotherapy. *Journal of neurosurgery*, *46*(2), 155–164.

Barkhausen, J., Ruehm, S. G., Goyen, M., Buck, T., Laub, G., & Debatin, J. F. (2001). MR evaluation of ventricular function: true fast imaging with steady-state precession versus fast low-angle shot cine MR imaging: feasibility study. *Radiology*, *219*(1), 264–9. doi:10.1148/radiology.219.1.r01ap12264

Berrington de González, A., & Darby, S. (2004). Risk of cancer from diagnostic X-rays: estimates for the UK and 14 other countries. *Lancet*, *363*(9406), 345–51. doi:10.1016/S0140-6736(04)15433-0

Center, M. B. I. (2010). BrainWeb: simulated brain database. Retrieved from http://brainweb.bic.mni.mcgill.ca/brainweb/

Chad Stickrath, M. (2012). Patient and Health Care Provider Discussions About the Risks of Medical Imaging. *ARCH INTERN MED*, *172*(13), 2012–2013.

Choong, M. K., Logeswaran, R., & Bister, M. (2007). Cost-effective handling of digital medical images in the telemedicine environment. *International journal of medical informatics*, *76*(9), 646–54. doi:10.1016/j.ijmedinf.2006.05.007

Cuadra, M. B., Cammoun, L., Butz, T., Cuisenaire, O., & Thiran, J. (2005). Comparison and Validation of Tissue Modelization and Statistical Classification Methods in T1-Weighted MR Brain Images. *IEEE TRANSACTIONS ON MEDICAL IMAGING*, *24*(12), 1548–1565.

Daniel X. Le, George R. Thoma, H. W. (1995). Classification of binary document images into textual or nontextual data blocks using neural network models. *Machine Vision and Applications*, *8*, 289–304.

De Leeuw, F. E., de Groot, J. C., Achten, E., Oudkerk, M., Ramos, L. M., Heijboer, R., … Breteler, M. M. (2001). Prevalence of cerebral white matter lesions in elderly people: a population based magnetic resonance imaging study. The Rotterdam Scan Study. *Journal of neurology, neurosurgery, and psychiatry*, *70*(1), 9–14. Retrieved from http://www.pubmedcentral.nih.gov/articlerender.fcgi?artid=1763449&tool=pmcentrez&rendertype=abstract

Duta, N., & Sonka, M. (1998). Segmentation and interpretation of MR brain images: an improved active shape model. *IEEE transactions on medical imaging*, *17*(6), 1049–62. doi:10.1109/42.746716

El-Dahshan, E.-S. A., Hosny, T., & Salem, A.-B. M. (2010). Hybrid intelligent techniques for MRI brain images classification. *Digital Signal Processing*, *20*(2), 433–441. doi:10.1016/j.dsp.2009.07.002

EL-SAYED A. EL-DAHSHAN, ABDEL-BADEEH M. SALEM, A. T. H. Y. (2009). A hybrid technique for automatic mri brain images classification. *STUDIA UNIV. BABES¸–BOLYAI, INFORMATICA*, *LIV*(1), 55–67.

Fan, J., Zeng, G., Body, M., & Hacid, M.-S. (2005). Seeded region growing: an extensive and comparative study. *Pattern Recognition Letters*, *26*(8), 1139–1156. doi:10.1016/j.patrec.2004.10.010

Fausett, L. (1994). Fundamentals of Neural Networks, Architecture, Algorithms and Applications. In *Prentice-Hall*.

Ferlay, J., Shin, H.-R., Bray, F., Forman, D., Mathers, C., & Parkin, D. M. (2010). Estimates of worldwide burden of cancer in 2008: GLOBOCAN 2008. *International journal of cancer. Journal international du cancer*, *127*(12), 2893–917. doi:10.1002/ijc.25516

Fischer, S., Šroubek, F., Perrinet, L., Redondo, R., & Cristóbal, G. (2007). Self-Invertible 2D Log-Gabor Wavelets. *International Journal of Computer Vision*, *75*(2), 231–246. doi:10.1007/s11263-006-0026-8

Fletcher-Heath, L. M., Hall, L. O., Goldgof, D. B., & Murtagh, F. R. (2001). *Automatic segmentation of non-enhancing brain tumors in magnetic resonance images. Artificial intelligence in medicine* (Vol. 21, pp. 43–63). Retrieved from http://www.ncbi.nlm.nih.gov/pubmed/11154873

Foster-Gareau, P., Heyn, C., Alejski, A., & Rutt, B. K. (2003). Imaging single mammalian cells with a 1.5 T clinical MRI scanner. *Magnetic resonance in medicine : official journal of the Society of Magnetic Resonance in Medicine / Society of Magnetic Resonance in Medicine*, *49*(5), 968–71. doi:10.1002/mrm.10417

Fung Kon Jin, P. H. P., Dijkgraaf, M. G. W., Alons, C. L., van Kuijk, C., Beenen, L. F. M., Koole, G. M., & Goslings, J. C. (2011). Improving CT scan capabilities with a new trauma workflow concept: simulation of hospital logistics using different CT scanner scenarios. *European journal of radiology*, *80*(2), 504–9. doi:10.1016/j.ejrad.2009.11.026

Gerhardt, W., J. Clausen, E. Christensen, and J. R. (1967). Lactate dehydrogenase isoenzymes in the diagnosis of human benign and malignant brain tumors. *Journal of the National Cancer Institute*, *38*(3).

Haykin, S. (1999). Neural network, A comprehensive Foundation, 2nd Edition.

He, W., Huda, W., Magill, D., Tavrides, E., & Yao, H. (2011). X-ray tube current modulation and patient doses in chest CT. *Radiation protection dosimetry*, *143*(1), 81–7. doi:10.1093/rpd/ncq291

Hyare, H., Wisco, J. J., Alusi, G., Cohen, M., Nabili, V., Abemayor, E., & Kirsch, C. F. E. (2010). The anatomy of nasopharyngeal carcinoma spread through the pharyngobasilar fascia to the trigeminal mandibular nerve on 1.5 T MRI. *Surgical and radiologic anatomy : SRA*, *32*(10), 937–44. doi:10.1007/s00276-010-0638-0

Jaffar, M. A., Zia, S., Latif, G., Mirza, A. M., & Mehmood, I. (2012). Anisotropic Diffusion based Brain MRI Segmentation and 3D Reconstruction. *International Journal of Computational Intelligence Systems*, (November), 37–41.

Kanungo, T., Member, S., Mount, D. M., Netanyahu, N. S., Piatko, C. D., Silverman, R., & Wu, A. Y. (2002). An Efficient k -Means Clustering Algorithm : Analysis and Implementation. *IEEE TRANSACTIONS ON PATTERN ANALYSIS AND MACHINE INTELLIGENCE*, *24*(7), 881–892.

Kaus, M. R., Warfield, S. K., Nabavi, a, Black, P. M., Jolesz, F. a, & Kikinis, R. (2001). Automated segmentation of MR images of brain tumors. *Radiology*, *218*(2), 586–91. Retrieved from http://www.ncbi.nlm.nih.gov/pubmed/11161183

Kikinis, R., & Pieper, S. (2011). 3D Slicer as a Tool for Interactive Brain Tumor Segmentation. *33rd Annual International Conference of the IEEE EMBS Boston, Massachusetts USA*, 6982–6984.

Kleihues, P., & Sobin, L. H. (2000). World Health Organization classification of tumors. *International Agency for Research on Cancer*, *88*(12), 2887. Retrieved from http://www.ncbi.nlm.nih.gov/pubmed/10870076

Knopp, M. V, Runge, V. M., Essig, M., Hartman, M., Jansen, O., Kirchin, M. A., … Lodemann, K. (2004). Radiology Primary and Secondary Brain Tumors at MR

Imaging : Bicentric Intraindividual Crossover Comparison of Gadobenate Dimeglumine and. *Neuroradiology*, *230*(1), 55–64.

Kohler, B. a, Ward, E., McCarthy, B. J., Schymura, M. J., Ries, L. a G., Eheman, C., … Edwards, B. K. (2011). Annual report to the nation on the status of cancer, 1975-2007, featuring tumors of the brain and other nervous system. *Journal of the National Cancer Institute*, *103*(9), 714–36. doi:10.1093/jnci/djr077

Kong, W. K., Zhang, D., & Li, W. (2003). Palmprint feature extraction using 2-D Gabor filters. *Pattern Recognition*, *36*(10), 2339–2347. doi:10.1016/S0031-3203(03)00121-3

Kovalev, V. a, Kruggel, F., Gertz, H. J., & von Cramon, D. Y. (2001). Three-dimensional texture analysis of MRI brain datasets. *IEEE transactions on medical imaging*, *20*(5), 424–33. doi:10.1109/42.925295

Kovesi, P. (2000). Phase congruency: a low-level image invariant. *Psychological research*, *64*(2), 136–48. Retrieved from http://www.ncbi.nlm.nih.gov/pubmed/11195306

Lahmiri, S. (2011). Brain MRI Classification using an Ensemble System and LH and HL Wavelet Sub-bands Features. *Computational Intelligence In Medical Imaging (CIMI)*, 1–7.

Liew, A., & Yan, H. (2006). Current Methods in the Automatic Tissue Segmentation of 3D Magnetic Resonance Brain Images. *Current Medical Imaging Reviews*, *2*(1), 91–103. doi:10.2174/157340506775541604

Liu, C., & Wechsler, H. (2002). Gabor feature based classification using the enhanced fisher linear discriminant model for face recognition. *IEEE transactions on image processing : a publication of the IEEE Signal Processing Society*, *11*(4), 467–76. doi:10.1109/TIP.2002.999679

Lu, D., & Weng, Q. (2007). A survey of image classification methods and techniques for improving classification performance. *International Journal of Remote Sensing*, *28*(5), 823–870. doi:10.1080/01431160600746456

M. Flaum, M. Sonka, S. Arndt, T. Cizadlo, S. Stoneall, and N. C. A. (1995). A new automated method of identifying neuroanatomic regions of interest on imaging data. In *Proc 34th Annu. Meet. American College of Neuropsychopharmacology* (p. p. 233).

Ma, W. Y., & Manjunath, B. S. (1995). A comparison of wavelet transform features for texture image annotation. *Proceedings., International Conference on Image Processing*, *2*, 256–259. doi:10.1109/ICIP.1995.537463

Maitra, M., & Chatterjee, A. (2008). Hybrid multiresolution Slantlet transform and fuzzy c-means clustering approach for normal-pathological brain MR image segregation. *Medical engineering & physics*, *30*(5), 615–23. doi:10.1016/j.medengphy.2007.06.009

Manjunath, B. S., & Ma, W. Y. (1996). Texture features for browsing and retrieval of image data. *IEEE Transactions on Pattern Analysis and Machine Intelligence*, *18*(8), 837–842. doi:10.1109/34.531803

Maria-Luiza Antonie, Osmar R. Zaıane, A. C. (2006). Application of Data Mining Techniques for Medical Image Classification. *MDM/KDD'7*, 94–101.

Marroquin, J. L., Vemuri, B. C., Botello, S., & Calderon, F. (2002). An Accurate and Efficient Bayesian Method for Automatic Segmentation of Brain MRI. *IEEE TRANSACTIONS ON MEDICAL IMAGING*, *21*(8), 934–945.

Martinez-Möller, A., Souvatzoglou, M., Delso, G., Bundschuh, R. a, Chefd'hotel, C., Ziegler, S. I., … Nekolla, S. G. (2009). Tissue classification as a potential approach for attenuation correction in whole-body PET/MRI: evaluation with PET/CT data.

Journal of nuclear medicine : official publication, Society of Nuclear Medicine, *50*(4), 520–6. doi:10.2967/jnumed.108.054726

Materka, A. (2001). DISCRETE WAVELET TRANSFORM – DERIVED FEATURES FOR DIGITAL IMAGE TEXTURE ANALYSIS. *Proc. of Interational Conference on Signals and Electronic Systems*, (September), 163–168.

Materka, A., & Strzelecki, M. (1998). Texture Analysis Methods – A Review. *Technical university of lodz, institute of electronics, COST B11 report, Brussels*, 1–33.

MathWorks. (2012). Matlab.

Mesrob, L., Sarazin, M., Hahn-barma, V., Souza, L. C. De, Dubois, B., Gallinari, P., & Kinkingnéhun. (2012). DTI and Structural MRI Classification in Alzheimer ' s Disease. *Advances in Molecular Imaging*, *2*, 12–20. doi:10.4236/ami.2012.22003

Mitchell, Tom M. (1997). Bayesian Learning. In *Machine Learning* (pp. 154–178).

Mitchell, T. (1997). Machine Learning.

MRI, B. (2013). Abrar MRI Center.

Neubeck, a., & Van Gool, L. (2006). Efficient Non-Maximum Suppression. *18th International Conference on Pattern Recognition (ICPR'06)*, 850–855. doi:10.1109/ICPR.2006.479

O'Gorman, L., & Sanderson, a C. (1984). The converging squares algorithm: an efficient method for locating peaks in multidimensions. *IEEE transactions on pattern analysis and machine intelligence*, *6*(3), 280–8. Retrieved from http://www.ncbi.nlm.nih.gov/pubmed/21869194

Ocosco, C. H. A. C., Ollokian, V. A. K., Wan, R. E. M. I. K. K., Ike, G. B. R. P., & Vans, A. L. A. N. C. E. (1996). BrainWeb : Online Interface to a 3D MRI Simulated Brain Database. *Nature reviews neuroscience*, *2359*(3), 2359.

Omolara, K. A. (2011). Feasible Cancer Control Strategies for Nigeria : *American Journal of TROPICAL MEDICINE & Public Health*, *1*(1), 1–10.

Palo, S., & Alto, P. (1988). Snakes : Active Contour Models. *International Journal of Computer Vision*, *331*, 321–331.

Pang, B., & Lee, L. (2008). Opinion Mining and Sentiment Analysis. (C. C. Aggarwal & C. Zhai, Eds.)*Foundations and Trends® in Information Retrieval*, *2*(2), 1–135. doi:10.1561/1500000001

Perona, P., & Malik, J. (1990). Scale-space and edge detection using anisotropic diffusion. *IEEE Transactions on Pattern Analysis and Machine Intelligence*, *12*(7), 629–639. doi:10.1109/34.56205

Pichler, B. J., Kolb, A., Nägele, T., & Schlemmer, H.-P. (2010). PET/MRI: paving the way for the next generation of clinical multimodality imaging applications. *Journal of nuclear medicine : official publication, Society of Nuclear Medicine*, *51*(3), 333–6. doi:10.2967/jnumed.109.061853

Pietka, E. (1994). Lung segmentation in digital radiographs. *Journal of digital imaging*, *7*(2), 79–84. Retrieved from http://www.ncbi.nlm.nih.gov/pubmed/8075188

Quratulain, Latif, G., Kazmi, S. B., Jaffar, M. A., & Mirza, A. M. (2010). Classification and Segmentation of Brain Tumor using Texture Analysis. *RECENT ADVANCES in ARTIFICIAL INTELLIGENCE, KNOWLEDGE ENGINEERING and DATA BASES*, 147–155.

R.C. Gonzalez, R. E. W. (2008). Wavelet and multi resoution processing,Digital Image Processing, *3rd editio*.

R.O. Duda, P.E. Hart, and D. G. S. (2001). Pattern classification. In *John Wiley and Sons*.

Raaymakers, B. W., Lagendijk, J. J. W., Overweg, J., Kok, J. G. M., Raaijmakers, a J. E., Kerkhof, E. M., … Brown, K. J. (2009). Integrating a 1.5 T MRI scanner with a 6

MV accelerator: proof of concept. *Physics in medicine and biology*, *54*(12), N229–37. doi:10.1088/0031-9155/54/12/N01

Rosset, A., Spadola, L., & Ratib, O. (2004). OsiriX: an open-source software for navigating in multidimensional DICOM images. *Journal of digital imaging*, *17*(3), 205–16. doi:10.1007/s10278-004-1014-6

Salat, D. H., Chen, J. J., van der Kouwe, a J., Greve, D. N., Fischl, B., & Rosas, H. D. (2011). Hippocampal degeneration is associated with temporal and limbic gray matter/white matter tissue contrast in Alzheimer's disease. *NeuroImage, 54*(3), 1795–802. doi:10.1016/j.neuroimage.2010.10.034

Singh, S. K., Clarke, I. D., Terasaki, M., Bonn, V. E., Hawkins, C., Squire, J., & Dirks, P. B. (2003). Identification of a Cancer Stem Cell in Human Brain Tumors Identification of a Cancer Stem Cell in Human Brain Tumors. *Cancer Research*, (63), 5821–5828.

Sun, G., Dong, X., & Xu, G. (2006). Tumor tissue identification based on gene expression data using DWT feature extraction and PNN classifier. *Neurocomputing*, *69*(4-6), 387–402. doi:10.1016/j.neucom.2005.04.005

Toma-Dasu, I., Uhrdin, J., Antonovic, L., Dasu, A., Nuyts, S., Dirix, P., … Brahme, A. (2012). Dose prescription and treatment planning based on FMISO-PET hypoxia. *Acta oncologica (Stockholm, Sweden)*, *51*(2), 222–30. doi:10.3109/0284186X.2011.599815

Volpe, J. J. (2009). Brain injury in premature infants: a complex amalgam of destructive and developmental disturbances. *Lancet neurology*, *8*(1), 110–24. doi:10.1016/S1474-4422(08)70294-1

Wells, W. M., Grimson, W. L., Kikinis, R., & Jolesz, F. a. (1996). Adaptive segmentation of MRI data. *IEEE transactions on medical imaging*, *15*(4), 429–42. doi:10.1109/42.511747

Xu, Y., & Song, F. (2008). FEATURE EXTRACTION BASED ON A LINEAR SEPARABILITY CRITERION. *nternational Journal of Innovative Computing, Information and Control*, *4*(4), 2008.

YAKAMI. (2012). YAKAMI DICOM Tools.

Yang, X., & Fei, B. (2011). A multiscale and multiblock fuzzy C-means classification method for brain MR images. *Medical Physics*, *38*(6), 2879. doi:10.1118/1.3584199

Yu, C., Ruppert, G. C. S., & Nguyen, D. T. D. (2012). Statistical Asymmetry-based Brain Tumor Segmentation from 3D MR Images. *Proc. of the Intl. Conf. on Bio-inspired Systems and Signal Processing (BIOSIGNALS), SciTePress*, 978–989.

Yu, Y., & Acton, S. T. (2002). Speckle reducing anisotropic diffusion. *IEEE transactions on image processing : a publication of the IEEE Signal Processing Society*, *11*(11), 1260–70. doi:10.1109/TIP.2002.804276

Zehra, W., Hazir, T., Nisar, Y. B., Krishin, J., Azam, M., & Hassan, M. (2003). JPMA (Journal Of Pakistan Medical Association) Vol 53 , No . 10 , Oct 2003 Widespread Skeletal Tuberculosis in a two years old Girl, *53*(10), 41–42.

Zhang, H., Fritts, J. E., & Goldman, S. a. (2005). <title>A fast texture feature extraction method for region-based image segmentation</title>. (A. Said & J. G. Apostolopoulos, Eds.)*In Proc. SPIE*, *vol. 56*(85), 957–968. doi:10.1117/12.587899

Zhang, Y, Brady, M., & Smith, S. (2001). Segmentation of brain MR images through a hidden Markov random field model and the expectation-maximization algorithm. *IEEE transactions on medical imaging*, *20*(1), 45–57. doi:10.1109/42.906424

Zhang, Yudong, Dong, Z., Wu, L., & Wang, S. (2011). A hybrid method for MRI brain image classification. *Expert Systems with Applications*, *38*(8), 10049–10053. doi:10.1016/j.eswa.2011.02.012

Vitae

Name   : Ghazanfar Latif

Nationality   : Pakistani

Date of Birth   : 11/25/1988

 Email   : ghazanfar.latif@nu.edu.pk

Address   : Islamabad, Pakistan

Academic Background   : Received Bachelor of Science (BS) in Computer Science from National University of Computer and Emerging Sciences, Islamabad (Pakistan) in 2010 with CGPA of 3.41 out of 4.

Publications

1. International journal paper published named "Anisotropic Diffusion based Brain MRI Segmentation and 3D Reconstruction", International Journal of Computational Intelligence Systems Volume 5, Issue 3, 2012, pages 494-504.

2. International research paper published named "Classification and Segmentation of Brain Tumor using Texture Analysis" in International Conference on Artificial Intelligence, Knowledge Engineering and Databases (AIKED2010), University of Cambridge UK Pages: 147-155, ISBN ~ ISSN:1790-5109 , 978-960-474-154-0.